Shortcut to finite-time memory erasure

Geng Li [1,2] and Hui Dong[1,*]

[1]*Graduate School of China Academy of Engineering Physics, Beijing 100193, China*
[2]*School of Systems Science, Beijing Normal University, Beijing 100875, China*

To achieve fast computation, it is crucial to reset the memory to a desired state within a limited time. However, the inherent delay in the system's response often prevents reaching the desired state once the control process is completed in finite time. To address this challenge, we propose a shortcut strategy that incorporates an auxiliary control to guide the system towards an equilibrium state that corresponds to the intended control, thus enabling memory reset to desired accuracy regardless of the erasure speed. Through the application of thermodynamic geometry, we derive an optimal shortcut protocol for erasure processes that minimizes the energy cost. This research provides an effective design principle for realizing the finite-time erasure process to desired accuracy while simultaneously reducing the energy cost, thereby alleviating the burden of heat dissipation.

I. INTRODUCTION

Memory erasure is an essential step in computations with an unavoidable energy cost. Landauer's principle posts a fundamental lower bound on the energy cost of erasing a one-bit memory carried out infinitely slowly [1–3]. However, accelerating computing processes typically requires to complete memory erasure in finite time. There is a general trade-off between erasure speed and accuracy when rapidly initializing the memory system. In such a finite-time thermodynamic process, a system often does not immediately respond to external perturbation, resulting in a lag between the final state and the desired equilibrium state [4,5]. This systematic state lag poses a significant challenge in initializing the system promptly [6–12] with desired accuracy, and also leads to a substantial increase in energy costs when the erasure time is reduced [13–23]. The quest to achieve rapid and accurate erasure with minimal energy costs drives us to design alternative memory erasure strategies.

Much effort has been devoted to reduce the state lag developed in nonequilibrium driving processes [24–32]. An important strategy is to remove the final state lag for overdamped systems by inversely engineering the potential landscape with a continuous infinity of control parameters [10,28,33–35]. However, there still lack efficient strategies for reducing the state lag in general underdamped systems [31,32], especially for the memory erasure procedure [20,36]. As a promising candidate, shortcut to isothermality was proposed as a finite-time driving strategy to escort the system evolving along a series of instantaneous equilibrium states with limited control parameters [30]. Such a shortcut strategy has been applied to realize fast transitions between equilibrium states [37,38], improve free energy calculations [39,40], and design Brownian heat engines [41–44]. As shown in

Fig. 1, we adopt such shortcut strategy to design a finite-time erasure protocol to reset a classical memory. We demonstrate that the desired erasure accuracy is achievable with the sufficiently precise shortcut strategy, regardless of the erasure speed. The thermodynamic geometric approach [45–47] is used to design the optimal protocol with the minimal energy cost.

II. SHORTCUTS TO MEMORY ERASURE

The memory as a binary system can be simplified as a particle in a bistable potential well [1,2,48]. Here, we consider a one-bit memory system modeled by a Brownian particle in a double-well potential $U_o(x, \vec{\lambda}) = kx^4 - A\lambda_1 x^2 - B\lambda_2 x$, where x represents the coordinate. And k, A, and B are constant coefficients introduced to define the dimensionless variables $\vec{\lambda}(t) \equiv (\lambda_1, \lambda_2)$ as time-dependent control parameters. The evolution of the system is described by Hamiltonian $H_o(x, p, \vec{\lambda}) \equiv p^2/(2m) + U_o(x, \vec{\lambda})$ with p as the momentum and m as the mass of the particle. The memory is encoded by mapping the microstate x into two macrostates. If the particle is in the left well ($x < 0$), the system is in macrostate "0". Conversely, if the particle is in the right well ($x > 0$), the system is in macrostate "1", which serves as the blank state for storing memory.

The system is in contact with a thermal reservoir with a constant temperature T. The barrier separating the double well is assumed to be much larger than the thermal fluctuation so that the memory can be considered stable [6,8].

The particle initially follows an equilibrium distribution with the control parameters $\vec{\lambda}(0) = (1, 0)$ and is equally likely to stay in each macrostate (0 or 1) with the probabilities $P_0 = P_1 = 1/2$. The entropy is defined as $S \equiv -k_B \sum_{i=1}^{2} P_i \ln P_i = k_B \ln 2$ for the initial memory state with k_B being the Boltzmann constant. During the Landauer's quasistatic erasure process [1–3], the particle is expelled into macrostate "1" by varying control parameters $\vec{\lambda}$ slowly to

(a)   Conventional memory erasure $H = H_o$

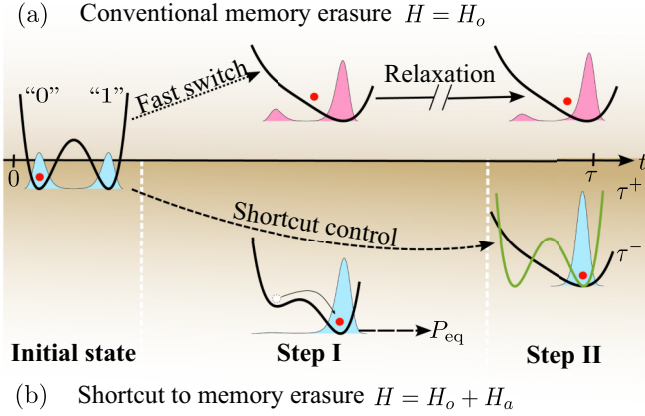(b)   Shortcut to memory erasure $H = H_o + H_a$

FIG. 1. Schematic of finite-time memory erasure. The one-bit memory is modeled by a physical double-well system. In the initial state, the system stores the state's information "0" or "1". The task of memory erasure is to reset the system into the blank state "1". (a) Conventional memory erasure scheme with the Hamiltonian H_o. The double-well potential is fast switched to fulfill classical memory reset in finite time τ. A systematic state lag is accumulated between the system's current state and its corresponding equilibrium state. Therefore, a slow relaxation process is needed to reach the desired erasure accuracy. (b) Shortcut to memory erasure with the Hamiltonian $H = H_o + H_a$. In the step I, an auxiliary Hamiltonian H_a is added to escort the system evolving along the instantaneous equilibrium path of the original Hamiltonian H_o within finite time. The system is finally expelled into the blank state "1" without accumulation of the state lag. In the step II, the potential is quenched to the double-well form (from τ^- to τ^+) for later computations.

maintain the equilibrium state $P_{eq} = \exp[\beta(F - H_o)]$, where $F \equiv -\beta^{-1} \ln[\iint dx dp \exp(-\beta H_o)]$ is the free energy with the inverse temperature $\beta \equiv 1/(k_B T)$. And the probabilities for the final memory state are $P_0 = 0$ and $P_1 = 1$ with the corresponding entropy $S = 0$. Such reduction of the entropy makes the memory erasure a logically irreversible process. Once the control parameters $\vec{\lambda}$ are tuned with finite rate as illustrated in Fig. 1(a), the system is driven to a nonequilibrium state typically with a lag, resulting in a residual entropy $S > 0$. And additional relaxation is required to achieve the desired accuracy with the sacrifice of erasure time [3,48,49].

To meet the need of fast erasure and reduce the lag, we adopt the shortcut scheme where an auxiliary Hamiltonian $H_a(x, p, t)$ is supplemented to escort the system evolving along the instantaneous equilibrium state P_{eq} during the finite-time erasure process with boundary conditions $H_a(0) = H_a(\tau) = 0$. The probability distribution $P(x, p, t)$ of the microstate follows the Kramers equation,

$$\frac{\partial P}{\partial t} = -\frac{\partial}{\partial x}\left(\frac{\partial H}{\partial p}P\right) + \frac{\partial}{\partial p}\left(\frac{\partial H}{\partial x}P + \gamma\frac{\partial H}{\partial p}P\right) + \frac{\gamma}{\beta}\frac{\partial^2 P}{\partial p^2},$$
(1)

where $H \equiv H_o + H_a$ is the total Hamiltonian and γ is the dissipation coefficient. Our operation of memory erasure, illustrated in Fig. 1(b), consists of two steps as follows.

Step I, Shortcut Erasure. The particle is expelled to the right well ($x > 0$) in the finite-time interval $t \in [0, \tau]$, by raising the left well, illustrated as the step I in Fig. 1(b).

The control parameters are tuned from $\vec{\lambda}(0)$ to $\vec{\lambda}(\tau) = (0, 1)$. With the strategy of shortcuts to isothermality [30], the system evolves along the path of instantaneous equilibrium states, and reaches the final equilibrium state $P = P_{eq}(\tau)$ with the control parameters $\vec{\lambda}(\tau)$. The requirement for the auxiliary Hamiltonian H_a follows as

$$\frac{\gamma}{\beta}\frac{\partial^2 H_a}{\partial p^2} - \frac{\gamma p}{m}\frac{\partial H_a}{\partial p} + \frac{\partial H_a}{\partial p}\frac{\partial H_o}{\partial x} - \frac{p}{m}\frac{\partial H_a}{\partial x} = \frac{dF}{dt} - \frac{\partial H_o}{\partial t}.$$
(2)

The auxiliary Hamiltonian is proved to have the form [30] $H_a(x, p, t) = \dot{\vec{\lambda}} \cdot \vec{f}(x, p, \vec{\lambda})$ with details presented in Appendix A. Extra boundary conditions $\dot{\vec{\lambda}}(0) = \dot{\vec{\lambda}}(\tau) = 0$ are imposed to ensure that the auxiliary control vanishes at the beginning and end of the erasure process.

Step II, Potential Quench. For later computation purpose, the potential is reset to the double-well form. Such operation is realized by quenching the control parameters from $\vec{\lambda}(\tau^-) = (0, 1)$ to the initial value $\vec{\lambda}(\tau^+) = (1, 0)$ at the time $t = \tau$ with an instantaneous change of the system Hamiltonian $H_o(\tau^-) \to H_o(\tau^+)$. Here, τ^- and τ^+ denote the time before and after the potential quench, respectively.

After these two steps, the memory is erased to the blank state and the system is reset within finite time τ to allow the later usage. It is worth noting that the erasure accuracy, denoted by $\epsilon \equiv \int_0^\infty dx \int_{-\infty}^{+\infty} dp P(x, p, \tau)$, remains constant for the shortcut strategy, irrespective of the erasure duration τ. This constancy holds because the distribution of the final blank state, $P(x, p, \tau) = P_{eq}(x, p, \vec{\lambda}(\tau))$, remains independent of the erasure duration τ with the implementation of a reducible control protocol, represented by $\vec{\lambda}(t) = \vec{\lambda}(t/\tau)$ with the reducible time t/τ varying from 0 to 1. We remark that we choose the final parameter $\vec{\lambda}(\tau) = (0, 1)$ based on the experimental simplicity of the scheme while ensuring the erasure accuracy ϵ.

III. GEOMETRIC ERASURE PROTOCOL

Energy cost is inevitable in a finite-time erasure process. We employ the geometric approach [45,46] to derive the optimal erasure protocol with minimal energy costs. In the shortcut scheme with the total Hamiltonian $H = H_o + H_a$, the work performed in the erasure process with duration τ is $W_s \equiv \langle \int_0^\tau \partial H/\partial t\, dt \rangle_{eq}$, which is explicitly obtained as

$$W_s = \Delta F_s + \gamma \int_0^\tau dt \left\langle \left(\frac{\partial H_a}{\partial p}\right)^2 \right\rangle_{eq},$$
(3)

where $\langle \cdot \rangle_{eq} \equiv \iint dx dp [\cdot] P_{eq}$ and ΔF_s is the free energy difference in Step I. Details are presented in Appendix B. Since the potential quench in the Step II is realized instantaneously, the system distribution remains unchanged. And the work done in this process follows as $W_q \equiv \iint dx dp (H_o(\tau^+) - H_o(\tau^-)) P_{eq}(\tau)$.

With the explicit form of the auxiliary Hamiltonian $H_a = \dot{\vec{\lambda}} \cdot \vec{f}$, the irreversible energy cost of the erasure process is written as

$$W_{irr} \equiv W - \Delta F_s - \Delta F_q$$

$$= \gamma \sum_{\mu\nu} \int_0^\tau dt\, \dot{\lambda}_\mu \dot{\lambda}_\nu \left\langle \frac{\partial f_\mu}{\partial p}\frac{\partial f_\nu}{\partial p} \right\rangle_{eq} + W_q - \Delta F_q,$$
(4)

where $W = W_s + W_q$ represents the total work and ΔF_q is the free energy difference in Step II. Here, the irreversible work in the quench step $W_q - \Delta F_q$ is settled when the starting state $P_{eq}(\tau)$ and the ending control $(1,0)$ are given. Therefore, we only need to consider the optimization of the irreversible work in the erasure step, $\gamma \sum_{\mu\nu} \int_0^\tau dt \dot{\lambda}_\mu \dot{\lambda}_\nu \langle (\partial f_\mu/\partial p)(\partial f_\nu/\partial p) \rangle_{eq}$. In the space of the control parameters $\vec{\lambda}$, a semi-positive metric can be defined as $g_{\mu\nu} \equiv \gamma \langle (\partial f_\mu/\partial p)(\partial f_\nu/\partial p) \rangle_{eq}$ on a Riemannian manifold. The shortest curve connecting two given endpoints in this parametric space is the geodesic line with the distance described by the thermodynamic length [50–53] $\mathcal{L} \equiv \int_0^\tau dt \sqrt{\sum_{\mu\nu} \dot{\lambda}_\mu \dot{\lambda}_\nu g_{\mu\nu}}$, which provides a lower bound for the irreversible energy cost $W_{irr} \geqslant \mathcal{L}^2/\tau$. Therefore, the geodesic protocol stands as the optimal erasure protocol with minimal energy costs. Utilizing the Riemannian metric $g_{\mu\nu}$, we derive the geodesic protocol by solving the geodesic equation: $\ddot{\lambda}_\mu + \sum_{\nu\kappa} \Gamma^\mu_{\nu\kappa} \dot{\lambda}_\nu \dot{\lambda}_\kappa = 0$, where the Christoffel symbol follows as $\Gamma^\mu_{\nu\kappa} \equiv \sum_\iota (g^{-1})_{\iota\mu} (\partial_{\lambda_\kappa} g_{\iota\nu} + \partial_{\lambda_\nu} g_{\iota\kappa} - \partial_{\lambda_\iota} g_{\nu\kappa})/2$.

In the shortcut scheme, the auxiliary Hamiltonian H_a is solved from Eq. (2) with the given original Hamiltonian H_o. However, the specific form of H_a typically relies on the particle's momentum [30,40,46]. The demand of constantly monitoring the particle's velocity makes it difficult for implementation of momentum-dependent terms in experiments [54,55]. To address this, we propose a variational auxiliary control $H_a^* = \dot{\vec{\lambda}} \cdot \vec{f}^*(x, p, \vec{\lambda})$ as an approximation to H_a. Here $\vec{f}^*$ approximates the function $\vec{f}$ to minimize a variational functional:

$$\mathcal{G}(H_a^*) = \int dx dp \left(\frac{\gamma}{\beta} \frac{\partial^2 H_a^*}{\partial p^2} - \frac{\gamma p}{m} \frac{\partial H_a^*}{\partial p} + \frac{\partial H_o}{\partial x} \frac{\partial H_a^*}{\partial p} \right.$$
$$\left. - \frac{p}{m} \frac{\partial H_a^*}{\partial x} + \frac{\partial H_o}{\partial t} - \frac{dF}{dt} \right)^2 e^{-\beta H_o}. \quad (5)$$

Such variational functional is defined to ensure the minimum deviation between evolutions governed by the approximate Hamiltonian H_a^* and the exact Hamiltonian H_a. To illustrate the shortcut scheme, we consider the variational auxiliary Hamiltonian $H_a^* = \sum_{\mu=1}^2 \dot{\lambda}_\mu f_\mu^*(x, p, \vec{\lambda})$ with two approximate tests: the quartic form with $f_1^* = a_1 xp + a_2 p + a_3 x^4 + a_4 x^3 + a_5 x^2 + a_6 x$, and $f_2^* = b_1 xp + b_2 p + b_3 x^4 + b_4 x^3 + b_5 x^2 + b_6 x$, and the quadratic form with $f_1^* = a_1 xp + a_2 p + a_3 x^2 + a_4 x$, and $f_2^* = b_1 xp + b_2 p + b_3 x^2 + b_4 x$, where $a_n \equiv a_n(\vec{\lambda})$ and $b_n \equiv b_n(\vec{\lambda})$ (with $n = 1, 2, 3, 4, 5, 6$) are functions to be determined through the variational procedure. Here we neglect the high-order momentum terms in the auxiliary Hamiltonian due to experimental challenges in continuously recording the particle's velocity [55]. We give an illustration of how this approximation works with an example in Appendix E. With the adoption of the shortcut scheme under the total Hamiltonian $H = H_o + H_a^*$, the system is anticipated to evolve along a series of near-equilibrium state $P_{eq}^* \approx P_{eq}$. This approximation will change the energy cost defined in Eq. (4) due to the approximate P_{eq}^* resulted from the form of the auxiliary control H_a^* in Eq. (5). The inclusion of higher-order and complex terms in H_a^* enables a closer path to equilibrium one for subsequent optimization procedures. Detailed discussions are presented in Appendixes C and H.

With the operation of a gauge transformation $X = x$ and $P = p + m\partial H_a^*/\partial p$, we obtain an equivalent process

$$\dot{X} = \frac{P}{m}, \quad \dot{P} = -\frac{\partial U_o}{\partial X} - \frac{\partial U_a}{\partial X} - \gamma \dot{X} + \xi(t), \quad (6)$$

where $\xi(t)$ is the Gaussian white noise and the momentum-independent auxiliary potential takes the quartic form $U_a = \dot{\lambda}_1 (a_3 X^4 + a_4 X^3 + a_5 X^2 + a_6 X) + \dot{\lambda}_2 (b_3 X^4 + b_4 X^3 + b_5 X^2 + b_6 X) + C_2(t)X^2 + C_1(t)X$ or the quadratic form $U_a = \dot{\lambda}_1 (a_3 X^2 + a_4 X) + \dot{\lambda}_2 (b_3 X^2 + b_4 X) + C_2(t)X^2 + C_1(t)X$. Detailed derivations of the equivalent process in Eq. (6) and the lengthy expressions of $C_1(t)$ and $C_2(t)$ are presented in Appendixes C and D. In this equivalent process, the fixed form of the system's distribution changes from $P_{eq}(x, p, \vec{\lambda})$ to the form

$$P_f(X, P, t) = \exp\left\{ \beta \left[F - \frac{1}{2m}(P - m\partial H_a^*/\partial P)^2 - U_o \right] \right\}. \quad (7)$$

With the boundary conditions $\dot{\vec{\lambda}}(0) = \dot{\vec{\lambda}}(\tau) = 0$, the extra term $m\partial H_a^*/\partial P = m\dot{\vec{\lambda}} \cdot \partial \vec{f}^*/\partial P$ with $H_a^* = \dot{\vec{\lambda}} \cdot \vec{f}^*$ in Eq. (7) vanishes and the system's distribution P_f returns to the instantaneous equilibrium distribution P_{eq}^* at the beginning $t = 0$ and end $t = \tau$ of the driving process.

IV. RESET ERRORS

The conventional approach of memory erasure is to tune the system Hamiltonian H_o via control parameters $\vec{\lambda}$. The memory state evolves accordingly yet with a lag, which induces reset errors especially for the case with short erasure time τ [31]. The shortcut scheme with the Hamiltonian $H = H_o + U_a$ effectively fulfills the demands for both erasure speed and accuracy, without further introducing additional freedom of control.

We numerically obtain the shortcut scheme with the Hamiltonian $H = H_o + U_a$ and compare it with the conventional scheme with the Hamiltonian $H' = H_o$ in a one-bit memory erasure process. In simulations, we choose the parameters as $k = 4$, $A = 8$, $B = 16$, $k_B T = 1$, $\gamma = 1$, and $m = 0.01$. A straightforward control protocol is selected as $\lambda_1^s(t) = 0.5 + 0.5 \cos(\pi t/\tau)$ and $\lambda_2^s(t) = 0.5 - 0.5 \cos(\pi t/\tau)$ to continuously meet the boundary conditions. Figure 2 shows the erasure accuracy ϵ for different erasure durations τ. The accuracy of the shortcut scheme is superior to that of the conventional scheme over different durations. Especially for the quartic shortcut scheme, the erasure accuracy maintains high accuracy in short erasure durations where the other two schemes fails. See Appendix H for more details about the simulation and examples with the polynomial protocol.

V. ENERGY COST OPTIMIZATION

In the shortcut scheme, the auxiliary Hamiltonian H_a^* is obtained once the control protocol $\vec{\lambda}(t)$ with $t \in [0, \tau]$ is specified for the conventional erasure process. Among various protocols, one with the minimum energy cost can be found with our geometric methods. We test the geometric approach for minimizing the energy cost of the erasure process. The geodesic protocol is obtained by numerically solving the geodesic equation in the parametric space $\vec{\lambda}$ with the metric
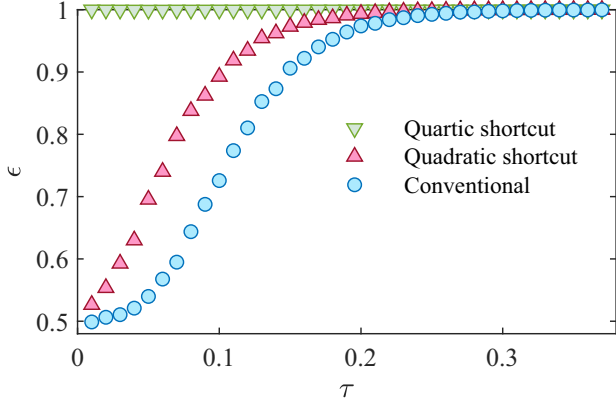
FIG. 2. The erasure accuracy ϵ of the quartic shortcut scheme (green inverted triangles), the quadratic shortcut scheme (red regular triangles), and the conventional erasure scheme (blue circles). The erasure accuracy is defined as the probability of particles ending in the right well $\epsilon \equiv \int_0^\infty dx \int_{-\infty}^{+\infty} dp P(x, p, \tau)$. During the erasure process, the shortcut scheme adopts the Hamiltonian $H = H_o + U_a$ while the conventional scheme takes the Hamiltonian $H' = H_o$. In the simulation, we choose the parameters as $k = 4$, $A = 8$, $B = 16$, $k_B T = 1$, $\gamma = 1$, and $m = 0.01$ and the straightforward control protocol as $\lambda_1^s(t) = 0.5 + 0.5\cos(\pi t/\tau)$ and $\lambda_2^s(t) = 0.5 - 0.5\cos(\pi t/\tau)$. In the simulated erasure durations, the quartic shortcut scheme always ensures high erasure accuracy while the quadratic shortcut scheme provides a larger erasure accuracy than that of the conventional erasure scheme.

$g_{\mu\nu}$. The details on the form of the metric and the geodesic equation are presented in Appendix F.

Figure 3(a) shows the difference between the geodesic protocol of the quartic shortcut scheme $\vec{\lambda}^{g,4}(t)$ (solid lines), the geodesic protocol of the quadratic shortcut scheme $\vec{\lambda}^{g,2}(t)$ (dot dash lines), and the straightforward protocol $\vec{\lambda}^s(t)$ (dash lines). Notably, both geodesic protocols $\vec{\lambda}^{g,4}(t)$ and $\vec{\lambda}^{g,2}(t)$ closely resemble a linear protocol with a constant rate, in contrast to the straightforward protocol $\vec{\lambda}^s(t)$.

In Fig. 3(b), we analyze the irreversible energy cost for the quartic shortcut scheme (inverted triangles and regular triangles), the quadratic shortcut scheme (squares and circles), and the conventional scheme (blue diamonds). The figure shows two main features. Firstly, the irreversible energy cost given by the geodesic protocol is lower than that from the straightforward protocol, particularly when we choose the approximate shortcut scheme (quartic or quadratic). This observation validates the effectiveness of the geometric approach for the shortcut scheme. Leveraging tools from Riemannian geometry [56], our two-step process significantly simplifies the search for the optimal erasure protocol. Secondly, we note that the quadratic shortcut scheme incurs a higher cost than the quartic shortcut scheme, aligning with the intuition that greater control freedom results in reduced energy costs. Figure 3(b) also shows that the approximate scheme with quartic shortcut can reduce energy cost comparing to the conventional scheme for the high accuracy at longer time. At the short time region, the cost of conventional scheme is low due to the low accuracy as shown in Fig. 2.
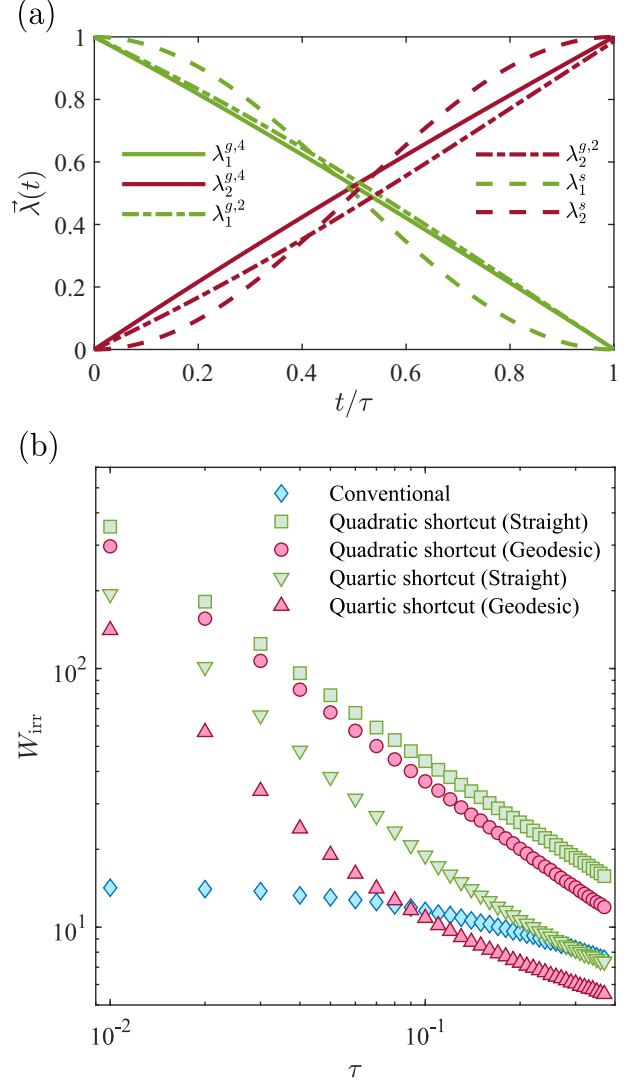

FIG. 3. (a) Geodesic protocol for the memory erasure process with the shortcut scheme. The control parameters vary from the initial value $\vec{\lambda}(0) = (1, 0)$ to the final value $\vec{\lambda}(\tau) = (0, 1)$. The solid lines represent the geodesic protocol of the quartic shortcut scheme $\vec{\lambda}^{g,4}(t)$; The dot dash lines represent the geodesic protocol of the quadratic shortcut scheme $\vec{\lambda}^{g,2}(t)$; The dash lines represent the straightforward protocol $\lambda_1^s(t) = 0.5 + 0.5\cos(\pi t/\tau)$ and $\lambda_2^s(t) = 0.5 - 0.5\cos(\pi t/\tau)$. The geodesic protocol is obtained by solving the geodesic equation corresponding to the metric $g_{\mu\nu}$. (b) The irreversible energy cost of the straightforward protocol (green) and the geodesic protocol (red) for the quartic shortcut scheme (inverted triangles and regular triangles), the quadratic shortcut scheme (squares and circles), and the conventional scheme (blue diamonds). The geodesic protocol for erasure processes demonstrates lower energy costs compared to the straightforward protocol.

VI. CONCLUSION AND REMARKS

In summary, we have developed a shortcut strategy to realize a finite-time one-bit memory erasure with minimal energy costs. In the shortcut scheme, an auxiliary control has been introduced to escort the system evolving along the path of instantaneous equilibrium states. We have employed the variational procedure to remove the momentum-dependent terms

and derive an accessible auxiliary control. The irreversible energy cost of the erasure process have been minimized by adopting the geometric method that connects the optimal erasure protocol with the geodesic protocol in a Riemannian manifold. This property helps us to solve the optimal protocol by using methods developed in geometry. Numerical results have verified that the shortcut strategy can largely improve the accuracy of finite-time memory erasure without further introducing additional control freedom. And a desired erasure accuracy can be achieved by increasing the control freedom of the auxiliary control. Our strategy shall provide an effective design principle for finite-time memory erasure with low energy costs.

Numerous studies have focused on minimizing the state lag in finite-time thermodynamic processes and enhancing erasure accuracy. These include the geometric optimization scheme [18], optimal transport scheme [10,11], and the shortcut to thermodynamic computing scheme [12]. However, previous studies have primarily focused on overdamped systems, leaving a gap in efficient strategies for improving erasure efficiency in underdamped systems. Our work addresses this void by introducing a versatile shortcut scheme applicable to both overdamped and underdamped systems. This contribution significantly advances erasure efficiency across a wider spectrum of thermodynamic processes.

Recently, much effort has been devoted to realize the one-bit memory erasure with quasi-static control strategies [7–9,20,57]. The state lag accumulated in a finite-rate operation hinders the development of finite-time erasure schemes. Our strategy offers an operable approach to eliminate the nonequilibrium lag and realize the finite-time memory erasure with high accuracy and low energy costs. Besides, the Landauer's bound have been approached in an underdamped micromechanical oscillator [20,36]. The fast equilibrium recovery strategy has also been achieved with a levitated particle in the underdamped regime [58]. The driving force in our shortcut scheme only depends on the particle's position. Therefore, it is promising to realize our finite-time memory erasure strategy with current experimental platforms.

ACKNOWLEDGMENTS

APPENDIX A: THE AUXILIARY CONTROL IN SHORTCUTS TO MEMORY ERASURE

In this Appendix, we will present details on the finite-time memory erasure with the approximate shortcut scheme, where the momentum-dependent terms in the auxiliary control are removed by employing a variational method and a gauge transformation.

1. Approximate shortcut scheme

We consider a one-bit memory system described by the Hamiltonian $H_o(x, p, \vec{\lambda}) \equiv p^2/(2m) + U_o(x, \vec{\lambda})$ with the modulated double-well potential $U_o(x, \vec{\lambda}) = kx^4 - A\lambda_1 x^2 - B\lambda_2 x$.

In the shortcut scheme, an auxiliary Hamiltonian H_a is added to escort the system evolving along the instantaneous equilibrium state $P_{eq} = \exp[\beta(F - H_o)]$ during the finite-time erasure process with prescribed boundary conditions $H_a(0) = H_a(\tau) = 0$. The probability distribution $P(x, p, t)$ of the microstate evolves according to the Kramers equation:

$$\frac{\partial P}{\partial t} = -\frac{\partial}{\partial x}\left(\frac{\partial H}{\partial p}P\right) + \frac{\partial}{\partial p}\left(\frac{\partial H}{\partial x}P + \gamma\frac{\partial H}{\partial p}P\right) + \frac{\gamma}{\beta}\frac{\partial^2 P}{\partial p^2}, \quad \text{(A1)}$$

where $H \equiv H_o + H_a$ represents the total Hamiltonian. The detailed derivation of the Kramers equation in the shortcut scheme is presented in Ref. [45]. With the demand of instantaneous equilibrium paths, we derive the evolution equation for the auxiliary control [30],

$$\frac{\partial P_{eq}}{\partial t} = -\frac{\partial}{\partial x}\left[\frac{\partial(H_o + H_a)}{\partial p}P_{eq}\right]$$
$$+ \frac{\partial}{\partial p}\left[\frac{\partial(H_o + H_a)}{\partial x}P_{eq} + \gamma\frac{\partial(H_o + H_a)}{\partial p}P_{eq}\right] + \frac{\gamma}{\beta}\frac{\partial^2 P_{eq}}{\partial p^2}, \quad \text{(A2)}$$

which is simplified as

$$\beta\left(\frac{dF}{dt} - \frac{\partial H_o}{\partial t}\right)P_{eq}$$
$$= -\frac{\partial}{\partial x}\left(\frac{\partial H_a}{\partial p}P_{eq}\right) + \frac{\partial}{\partial p}\left(\frac{\partial H_a}{\partial x}P_{eq} + \gamma\frac{\partial H_a}{\partial p}P_{eq}\right)$$
$$= \left(\beta\frac{\partial H_a}{\partial p}\frac{\partial H_o}{\partial x} - \frac{\beta}{m}p\frac{\partial H_a}{\partial x} + \gamma\frac{\partial^2 H_a}{\partial p^2} - \frac{\gamma\beta}{m}p\frac{\partial H_a}{\partial p}\right)P_{eq}. \quad \text{(A3)}$$

The equation for the auxiliary control is then obtained as

$$\frac{\gamma}{\beta}\frac{\partial^2 H_a}{\partial p^2} - \frac{\gamma p}{m}\frac{\partial H_a}{\partial p} + \frac{\partial H_a}{\partial p}\frac{\partial H_o}{\partial x} - \frac{p}{m}\frac{\partial H_a}{\partial x} = \frac{dF}{dt} - \frac{\partial H_o}{\partial t}. \quad \text{(A4)}$$

Considering the explicit time-dependence of the free energy $F = F(\vec{\lambda})$ and the Hamiltonian $H_o = H_o(x, p, \vec{\lambda})$ presented by the control parameters $\vec{\lambda} = \vec{\lambda}(t)$, we further derive that

$$\frac{\gamma}{\beta}\frac{\partial^2 H_a}{\partial p^2} - \frac{\gamma p}{m}\frac{\partial H_a}{\partial p} + \frac{\partial H_a}{\partial p}\frac{\partial H_o}{\partial x} - \frac{p}{m}\frac{\partial H_a}{\partial x}$$
$$= \sum_\mu \dot{\lambda}_\mu\left(\frac{dF}{d\lambda_\mu} - \frac{\partial H_o}{\partial\lambda_\mu}\right). \quad \text{(A5)}$$

Comparing both sides of Eq. (A5), we find that the auxiliary Hamiltonian takes the form $H_a(x, p, t) = \sum_\mu \dot{\lambda}_\mu f_\mu(x, p, \vec{\lambda})$ where $f_\mu(x, p, \vec{\lambda})$ satisfies

$$\frac{\gamma}{\beta}\frac{\partial^2 f_\mu}{\partial p^2} - \frac{\gamma p}{m}\frac{\partial f_\mu}{\partial p} + \frac{\partial f_\mu}{\partial p}\frac{\partial H_o}{\partial x} - \frac{p}{m}\frac{\partial f_\mu}{\partial x} = \frac{dF}{d\lambda_\mu} - \frac{\partial H_o}{\partial\lambda_\mu}. \quad \text{(A6)}$$

The boundary conditions of the auxiliary Hamiltonian $H_a(0) = H_a(\tau) = 0$ are satisfied with the requirement $\dot{\vec{\lambda}}(0) = \dot{\vec{\lambda}}(\tau) = 0$.

Given the challenging nature of solving Eq. (A4) for the auxiliary Hamiltonian H_a analytically, we employ a variational method [40,46] to obtain an approximate auxiliary

control $H_a^* = \dot{\vec{\lambda}} \cdot \vec{f}^*(x, p, \vec{\lambda})$, where $\vec{f}^*$ denotes an approximation to $\vec{f}$. In this variational shortcut scheme, a functional, derived from Eq. (A4), is used to assess the approximation of the auxiliary control H_a^*:

$$
\mathcal{G}(H_a^*) = \int dx dp \left(\frac{\gamma}{\beta} \frac{\partial^2 H_a^*}{\partial p^2} - \frac{\gamma p}{m} \frac{\partial H_a^*}{\partial p} + \frac{\partial H_o}{\partial x} \frac{\partial H_a^*}{\partial p} \right.
$$
$$
\left. - \frac{p}{m} \frac{\partial H_a^*}{\partial x} + \frac{\partial H_o}{\partial t} - \frac{dF}{dt} \right)^2 e^{-\beta H_o}. \quad (A7)
$$

The best possible form of the approximate auxiliary control is achieved from the variational equation $\delta \mathcal{G}(H_a^*)/\delta H_a^* = 0$.

However, another challenge arises in the underdamped shortcut scheme due to momentum-dependence in the auxiliary control. This dependency on momentum is hard to realize experimentally due to the necessity of constantly monitoring the particle's speed [54,55]. To address this, the variational method and a gauge transformation are employed to eliminate the momentum-dependent terms in the auxiliary control. We firstly remove high-order momentum-dependent terms. Assuming the variational auxiliary Hamiltonian linearly depends on momentum, it takes the form:

$$
H_a^* = \dot{\lambda}_1 f_1 + \dot{\lambda}_2 f_2, \quad (A8)
$$

where

$$
f_1(x, p, \vec{\lambda}) = a_1(\vec{\lambda}) x p + a_2(\vec{\lambda}) p + Z_1(x, \vec{\lambda}) \quad (A9)
$$

and

$$
f_2(x, p, \vec{\lambda}) = b_1(\vec{\lambda}) x p + b_2(\vec{\lambda}) p + Z_2(x, \vec{\lambda}). \quad (A10)
$$

The explicit forms of a_1, a_2, b_1, b_2, Z_1, and Z_2 will be determined in the variational procedure. We elaborate how the assumption of neglecting high-order momentum terms works in Sec. E. With the specified form of the auxiliary control

in Eqs. (A9) and (A10), the variational operation over H_a^* is transformed into a partial-derivative operation over parameters a_1, a_2, b_1, b_2, Z_1, and Z_2.

2. An equivalent process with a momentum-independent auxiliary control

Note that linear momentum-dependent terms persist in the variational auxiliary Hamiltonian in Eq. (A8). In the variational shortcut scheme employing the Hamiltonian $H = H_o + H_a^*$, the particle's evolution adheres to the Langevin equation

$$
\dot{x} = \frac{p}{m} + \dot{\lambda}_1(a_1 x + a_2) + \dot{\lambda}_2(b_1 x + b_2),
$$
$$
\dot{p} = -4kx^3 + 2A\lambda_1 x + B\lambda_2 - \dot{\lambda}_1 \left(a_1 p + \frac{\partial Z_1}{\partial x} \right)
$$
$$
- \dot{\lambda}_2 \left(b_1 p + \frac{\partial Z_2}{\partial x} \right) - \gamma \dot{x} + \xi(t), \quad (A11)
$$

where $\xi(t)$ represents the Gaussian white noise. However, the measurement difficulties associated with momentum-dependent forces in Eq. (A11) pose significant obstacles to practically implementing the shortcut scheme experimentally [54,55].

To circumvent this, a gauge transformation $X = x$ and $P = p + m\dot{\lambda}_1(a_1 x + a_2) + m\dot{\lambda}_2(b_1 x + b_2)$ is introduced to obtain an equivalent process with the variables X and P under the evolution as follows:

$$
\dot{X} = \frac{P}{m},
$$
$$
\dot{P} = -\frac{\partial U_o}{\partial X} - \frac{\partial U_a}{\partial X} - \gamma \dot{X} + \xi(t). \quad (A12)
$$

Here the auxiliary potential for these new variables follows as $U_a(X, t) = \dot{\lambda}_1 Z_1(X, t) + \dot{\lambda}_2 Z_2(X, t) + C_2(t) X^2 + C_1(t) X$ with the parameters

$$
C_2(t) = -\frac{m}{2} \left(\ddot{\lambda}_1 a_1 + \ddot{\lambda}_2 b_1 + \dot{\lambda}_1^2 \frac{\partial a_1}{\partial \lambda_1} + \dot{\lambda}_1^2 a_1^2 + \dot{\lambda}_2^2 \frac{\partial b_1}{\partial \lambda_2} + \dot{\lambda}_2^2 b_1^2 + \dot{\lambda}_1 \dot{\lambda}_2 \frac{\partial a_1}{\partial \lambda_2} + \dot{\lambda}_1 \dot{\lambda}_2 \frac{\partial b_1}{\partial \lambda_1} + 2\dot{\lambda}_1 \dot{\lambda}_2 a_1 b_1 \right),
$$
$$
C_1(t) = -m \left(\ddot{\lambda}_1 a_2 + \ddot{\lambda}_2 b_2 + \dot{\lambda}_1^2 \frac{\partial a_2}{\partial \lambda_1} + \dot{\lambda}_1^2 a_1 a_2 + \dot{\lambda}_2^2 \frac{\partial b_2}{\partial \lambda_2} + \dot{\lambda}_2^2 b_1 b_2 + \dot{\lambda}_1 \dot{\lambda}_2 \frac{\partial a_2}{\partial \lambda_2} + \dot{\lambda}_1 \dot{\lambda}_2 \frac{\partial b_2}{\partial \lambda_1} + \dot{\lambda}_1 \dot{\lambda}_2 a_2 b_1 + \dot{\lambda}_1 \dot{\lambda}_2 a_1 b_2 \right). \quad (A13)
$$

With the operation of Jacobi's transformation, we find that the system's distribution in this equivalent process follows a fixed form as

$$
P_f(X, P, t) = \exp \left\{ \beta \left[F - \frac{1}{2m}(P - m\partial H_a^*/\partial P)^2 - U_o \right] \right\}. \quad (A14)
$$

Comparing this fixed distribution P_f with the instantaneous equilibrium distribution $P_{eq} = \exp[\beta(F - H_o)]$, the extra term $m\partial H_a^*/\partial P$ with $H_a^* = \dot{\vec{\lambda}} \cdot \vec{f}^*$ within P_f vanishes at the beginning $t = 0$ and end $t = \tau$ times of the equivalent

process, considering the relation $\partial H_a^*/\partial P = \dot{\vec{\lambda}} \cdot \partial \vec{f}^*/\partial P$ and the boundary conditions $\dot{\vec{\lambda}}(0) = \dot{\vec{\lambda}}(\tau) = 0$. Consequently, the system's distribution P_f returns to the instantaneous equilibrium distribution P_{eq} at the beginning $t = 0$ and end $t = \tau$ of the equivalent process with the Hamiltonian $H = H_o + U_a$.

APPENDIX B: ENERGY COST OF A SHORTCUT TO MEMORY ERASURE PROCESS

This Appendix focuses on deriving the energy cost of the shortcut to memory erasure process. In the shortcut scheme with the Hamiltonian $H = H_o + H_a$, the stochastic trajectory

work [59,60] follows as

$$
\begin{aligned}
w[x(t), p(t)] &\equiv \int_0^\tau dt \frac{\partial H_o(x(t), p(t), \vec{\lambda})}{\partial t} + \int_0^\tau dt \frac{\partial H_a(x(t), p(t), t)}{\partial t} \\
&= \int_0^\tau dt \frac{\partial H_o(x(t), p(t), \vec{\lambda})}{\partial t} + \int_0^\tau dt \left(\frac{dH_a}{dt} - \dot{x}(t) \frac{\partial H_a}{\partial x} - \dot{p}(t) \frac{\partial H_a}{\partial p} \right) \\
&= \int_0^\tau dt \frac{\partial H_o(x(t), p(t), \vec{\lambda})}{\partial t} - \int_0^\tau dt \left(\dot{x}(t) \frac{\partial H_a(x(t), p(t), t)}{\partial x} + \dot{p}(t) \frac{\partial H_a(x(t), p(t), t)}{\partial p} \right).
\end{aligned}
\tag{B1}
$$

Here in the second line of Eq. (B1), we have considered the boundary conditions $\dot{\vec{\lambda}}(0) = \dot{\vec{\lambda}}(\tau) = 0$ which leads to $H_a(0) = H_a(\tau) = 0$. The average of the trajectory work (energy cost) is obtained as

$$
\begin{aligned}
W_s &\equiv \langle w \rangle_\xi = \iint D[x(t)]D[p(t)] \mathcal{T}[x(t), p(t)] w[x(t), p(t)] \\
&= \iint D[x(t)]D[p(t)] \mathcal{T}[x(t), p(t)] \int_0^\tau dt \iint dx dp \delta(x - x(t))\delta(p - p(t)) \\
&\quad \times \left[\frac{\partial H_o(x(t), p(t), \vec{\lambda})}{\partial t} - \left(\dot{x}(t) \frac{\partial H_a(\vec{x}(t), \vec{p}(t), t)}{\partial x} + \dot{p}(t) \frac{\partial H_a(x(t), p(t), t)}{\partial p} \right) \right] \\
&= \int_0^\tau dt \iint dx dp \left[\frac{\partial H_o(x, p, \vec{\lambda})}{\partial t} \langle \delta(x - x(t))\delta(p - p(t)) \rangle_\xi \right. \\
&\quad \left. - \left(\frac{\partial H_a(x, p, t)}{\partial x} \langle \dot{x}(t)\delta(x - x(t))\delta(p - p(t)) \rangle_\xi + \frac{\partial H_a(x, p, t)}{\partial p} \langle \dot{p}(t)\delta(x - x(t))\delta(p - p(t)) \rangle_\xi \right) \right] \\
&= \int_0^\tau dt \iint dx dp \left[\frac{\partial H_o(x, p, \vec{\lambda})}{\partial t} P(x, p, t) - \left(\frac{\partial H_a(x, p, t)}{\partial x} \langle \dot{x}(t)\rho(x, p, t) \rangle_\xi + \frac{\partial H_a(x, p, t)}{\partial p} \langle \dot{p}(t)\rho(x, p, t) \rangle_\xi \right) \right].
\end{aligned}
\tag{B2}
$$

Here $\mathcal{T}[x(t), p(t)]$ is the probability of the trajectory $[x(t), p(t)]$ associated with a noise realization $[\xi(t)]$. $\langle \cdot \rangle_\xi$ represents an average over different realizations of $[\xi]$. The system's distribution is defined as $P(x, p, t) \equiv \langle \rho(x, p, t) \rangle_\xi$, where $\rho(x, p, t) \equiv \delta(x - x(t))\delta(p - p(t))$ is the probability of a trajectory $[x(t), p(t)]$. In the shortcut scheme, the system follows the instantaneous equilibrium path with $P = P_{eq} = \exp[\beta(F - H_o)]$. Hence, the first part of the energy cost in Eq. (B2) is just the free energy difference [30] $\Delta F = \int_0^\tau dt \iint dx dp P_{eq} \partial_t H_o$. The irreversible energy cost is then computed as

$$
W_s \equiv \Delta F - \iint dx dp \int_0^\tau dt \left(\frac{\partial H_a(x, p, t)}{\partial x} \langle \dot{x}(t)\rho(x, p, t) \rangle_\xi + \frac{\partial H_a(x, p, t)}{\partial p} \langle \dot{p}(t)\rho(x, p, t) \rangle_\xi \right).
\tag{B3}
$$

With the Langevin equation

$$
\dot{x} = \frac{\partial H}{\partial p}, \quad \dot{p} = -\frac{\partial H}{\partial x} - \gamma \dot{x} + \xi(t),
\tag{B4}
$$

we calculate

$$
\begin{aligned}
\langle \dot{x}(t)\rho(x, p, t) \rangle_\xi &= \iint D[x(t)]D[p(t)] \mathcal{T}[x(t), p(t)] \dot{x}(t)\delta(x - x(t))\delta(p - p(t)) \\
&= \iint D[x(t)]D[p(t)] \mathcal{T}[x(t), p(t)] \delta(x - x(t))\delta(p - p(t)) \frac{\partial H(x(t), p(t), t)}{\partial p} \\
&= \frac{\partial H(x, p, t)}{\partial p} \iint D[x(t)]D[p(t)] \mathcal{T}[x(t), p(t)] \delta(x - x(t))\delta(p - p(t)) \\
&= \frac{\partial H(x, p, t)}{\partial p} P(x, p, t),
\end{aligned}
\tag{B5}
$$

and

$$
\begin{aligned}
\langle \dot{p}(t)\rho(x, p, t) \rangle_\xi &= \iint D[x(t)]D[p(t)] \mathcal{T}[x(t), p(t)] \dot{p}(t)\delta(x - x(t))\delta(p - p(t)) \\
&= \iint D[x(t)]D[p(t)] \mathcal{T}[x(t), p(t)] \delta(x - x(t))\delta(p - p(t)) \left(-\frac{\partial H(x(t), p(t), t)}{\partial x} - \gamma \dot{x}(t) + \xi(t) \right) \\
&= -\left(\frac{\partial H(x, p, t)}{\partial x} + \gamma \frac{\partial H(x, p, t)}{\partial p} \right) P(x, p, t) + \langle \xi(t)\rho(x, p, t) \rangle_\xi.
\end{aligned}
\tag{B6}
$$

With the consideration of the commutation between the stochastic force $\xi(t)$ and the coordinate x (the momentum p), we can obtain the relation [45,61]

$$\langle \xi(t)\rho(x, p, t)\rangle_\xi = -\gamma k_B T \frac{\partial}{\partial p} P(x, p, t). \tag{B7}$$

By leveraging these relations in Eqs. (B5), (B6), and (B7), we ultimately arrive at

$$
\begin{aligned}
W_s &= \Delta F - \int_0^\tau dt \iint dx dp \left[\frac{\partial H_a}{\partial x}\frac{\partial H}{\partial p}P_{eq} - \frac{\partial H_a}{\partial p}\left(\frac{\partial H}{\partial x}P_{eq} + \gamma\frac{\partial H}{\partial p}P_{eq} + \gamma k_B T\frac{\partial P_{eq}}{\partial p}\right)\right] \\
&= \Delta F - \int_0^\tau dt \iint dx dp \left[\frac{\partial H_a}{\partial x}\frac{\partial H_o}{\partial p} - \frac{\partial H_a}{\partial p}\frac{\partial H_o}{\partial x} - \gamma\left(\frac{\partial H_a}{\partial p}\right)^2\right]P_{eq} \\
&= \Delta F - \int_0^\tau dt \iint dx dp \left[-\frac{1}{\beta}\frac{\partial H_a}{\partial x}\frac{\partial P_{eq}}{\partial p} + \frac{1}{\beta}\frac{\partial H_a}{\partial p}\frac{\partial P_{eq}}{\partial x} - \gamma\left(\frac{\partial H_a}{\partial p}\right)^2 P_{eq}\right] \\
&= \Delta F - \int_0^\tau dt \iint dx dp \left[-\frac{1}{\beta}\frac{\partial}{\partial p}\left(\frac{\partial H_a}{\partial x}P_{eq}\right) + \frac{1}{\beta}\frac{\partial}{\partial x}\left(\frac{\partial H_a}{\partial p}P_{eq}\right) - \gamma\left(\frac{\partial H_a}{\partial p}\right)^2 P_{eq}\right] \\
&= \Delta F + \gamma \int_0^\tau dt \iint dx dp \left(\frac{\partial H_a}{\partial p}\right)^2 P_{eq}. \tag{B8}
\end{aligned}
$$

This expression matches the irreversible part of work given in Eq. (3) of the main text. In derivations of this result, we have taken integration by part and assumed that the boundary terms

$$\left(\frac{\partial H_a}{\partial x}P_{eq}\right)\bigg|_{p=+\infty} = \left(\frac{\partial H_a}{\partial x}P_{eq}\right)\bigg|_{p=-\infty} = 0,$$

and

$$\left(\frac{\partial H_a}{\partial p}P_{eq}\right)\bigg|_{x=+\infty} = \left(\frac{\partial H_a}{\partial p}P_{eq}\right)\bigg|_{x=-\infty} = 0.$$

APPENDIX C: APPROXIMATE FORM OF THE AUXILIARY CONTROL

The form of the auxiliary control still relies on the specific function representations of $Z_1(x, \vec{\lambda})$ and $Z_2(x, \vec{\lambda})$. In the following Appendix, we explore and present two approximate formulations for this auxiliary control.

1. Quartic form

Given the form of the double-well potential $U_o(x, \vec{\lambda}) = kx^4 - A\lambda_1 x^2 - B\lambda_2 x$, we assume quartic forms for the functions Z_1 and Z_2 in Eqs. (A9) and (A10) as

$$Z_1 = a_3 x^4 + a_4 x^3 + a_5 x^2 + a_6 x \tag{C1}$$

and

$$Z_2 = b_3 x^4 + b_4 x^3 + b_5 x^2 + b_6 x, \tag{C2}$$

where $a_n \equiv a_n(\vec{\lambda})$ and $b_n \equiv b_n(\vec{\lambda})$ with $n = 3, 4, 5, 6$ are functions to be determined through a variational procedure. Consequently, the auxiliary Hamiltonian becomes:

$$
\begin{aligned}
H_a^* &= \dot{\lambda}_1(a_1 xp + a_2 p + a_3 x^4 + a_4 x^3 + a_5 x^2 + a_6 x) \\
&\quad + \dot{\lambda}_2(b_1 xp + b_2 p + b_3 x^4 + b_4 x^3 + b_5 x^2 + b_6 x). \tag{C3}
\end{aligned}
$$

And the corresponding auxiliary potential takes the form as

$$
\begin{aligned}
U_a &= \dot{\lambda}_1(a_3 X^4 + a_4 X^3 + a_5 X^2 + a_6 X) + \dot{\lambda}_2(b_3 X^4 + b_4 X^3 \\
&\quad + b_5 X^2 + b_6 X) + C_2(t)X^2 + C_1(t)X, \tag{C4}
\end{aligned}
$$

where the parameters C_1 and C_2 are presented in Eq. (A13). Simulations indicate that the auxiliary Hamiltonian in Eq. (C3) or the auxiliary potential in Eq. (C4) enables perfect memory erasures without dependency on erasure duration τ. The detailed results of the simulation are shown in Fig. 2 of the main text. Compared with the original Hamiltonian H_o, the auxiliary potential U_a in Eq. (C4) adds two control freedoms, i.e., the X^4 term and the X^2 term.

2. Quadratic form

Given the double-well potential $U_o(x, \vec{\lambda}) = kx^4 - A\lambda_1 x^2 - B\lambda_2 x$ with two control parameters, we assume quadratic forms for Z_1 and Z_2:

$$Z_1 = a_3 x^2 + a_4 x \tag{C5}$$

and

$$Z_2 = b_3 x^2 + b_4 x, \tag{C6}$$

where $a_n \equiv a_n(\vec{\lambda})$ and $b_n \equiv b_n(\vec{\lambda})$ with $n = 3, 4$ are undetermined functions addressed through the variational procedure. Consequently, the auxiliary Hamiltonian and potential are given by

$$
\begin{aligned}
H_a^* &= \dot{\lambda}_1(a_1 xp + a_2 p + a_3 x^2 + a_4 x) \\
&\quad + \dot{\lambda}_2(b_1 xp + b_2 p + b_3 x^2 + b_4 x) \tag{C7}
\end{aligned}
$$

and

$$
\begin{aligned}
U_a &= \dot{\lambda}_1(a_3 X^2 + a_4 X) + \dot{\lambda}_2(b_3 X^2 + b_4 X) \\
&\quad + C_2(t)X^2 + C_1(t)X, \tag{C8}
\end{aligned}
$$

where the parameters C_1 and C_2 are described in Eq. (A13). Note that the auxiliary potential U_a in Eq. (C8) only depends on the X^2 term and the X term. The resulting shortcut strategy achieves erasure in finite time without introducing additional degrees of control means. As shown in Fig. 2 of the main text, the erasure accuracy of the auxiliary potential U_a in Eq. (C8) is superior to that of the conventional strategy across all simulated durations.

APPENDIX D: DIMENSIONLESS FORM OF THE ERASURE PROCESS

In this Appendix, we numerically solve the function $\vec{f}^*$ for the auxiliary control. To facilitate simulations, we introduce the characteristic length $l_c \equiv (k_B T/k)$, the characteristic times $\tau_1 = m/\gamma$ and $\tau_2 = \gamma/(kl_c^2)$ to define the dimensionless coordinate $\tilde{x} \equiv x/l_c$, momentum $\tilde{p} \equiv p\tau_2/(ml_c)$, time $s \equiv t/\tau_2$, and the parameters $\tilde{A} \equiv A/(kl_c^2)$ and $\tilde{B} \equiv B/(kl_c^3)$. The dimensionless evolution equation for the auxiliary control follows as

$$\frac{1}{\alpha^2}\frac{\partial^2 \tilde{H}_a}{\partial \tilde{p}^2} - \frac{\tilde{p}}{\alpha}\frac{\partial \tilde{H}_a}{\partial \tilde{p}} + \frac{1}{\alpha}\frac{\partial \tilde{H}_a}{\partial \tilde{p}}\frac{\partial \tilde{H}_o}{\partial \tilde{x}} - \tilde{p}\frac{\partial \tilde{H}_a}{\partial \tilde{x}} = \frac{d\tilde{F}}{ds} - \frac{\partial \tilde{H}_o}{\partial s}, \quad \text{(D1)}$$

with the dimensionless parameter $\alpha \equiv \tau_1/\tau_2$ and the dimensionless Hamiltonian $\tilde{H}_o \equiv H_o/(k_B T)$ and $\tilde{H}_a \equiv H_a/(k_B T)$. The dimensionless variational functional takes the form as

$$\tilde{\mathcal{G}}(\tilde{H}_a^*) = \int d\tilde{x}d\tilde{p}\left(\frac{1}{\alpha^2}\frac{\partial^2 \tilde{H}_a^*}{\partial \tilde{p}^2} - \frac{\tilde{p}}{\alpha}\frac{\partial \tilde{H}_a^*}{\partial \tilde{p}} + \frac{1}{\alpha}\frac{\partial \tilde{H}_a^*}{\partial \tilde{p}}\frac{\partial \tilde{H}_o}{\partial \tilde{x}}\right.$$
$$\left. - \tilde{p}\frac{\partial \tilde{H}_a^*}{\partial \tilde{x}} + \frac{\partial \tilde{H}_o}{\partial s} - \frac{d\tilde{F}}{ds}\right)^2 e^{-\tilde{H}_o}. \quad \text{(D2)}$$

In the following, we discuss respectively the quartic form and the quadratic form of the best possible auxiliary control $\tilde{H}_a^*$ through the variational procedure.

1. Dimensionless quartic form

Consider the quartic form of the auxiliary Hamiltonian in Eq. (C3). The dimensionless variational auxiliary Hamiltonian follows as

$$\tilde{H}_a^* = \lambda_1'(\tilde{a}_1\tilde{x}\tilde{p} + \tilde{a}_2\tilde{p} + \tilde{a}_3\tilde{x}^4 + \tilde{a}_4\tilde{x}^3 + \tilde{a}_5\tilde{x}^2 + \tilde{a}_6\tilde{x})$$
$$+ \lambda_2'(\tilde{b}_1\tilde{x}\tilde{p} + \tilde{b}_2\tilde{p} + \tilde{b}_3\tilde{x}^4 + \tilde{b}_4\tilde{x}^3 + \tilde{b}_5\tilde{x}^2 + \tilde{b}_6\tilde{x}), \quad \text{(D3)}$$

where $\lambda_1' \equiv d\lambda_1/ds$, $\lambda_2' \equiv d\lambda_2/ds$ and the parameters $\tilde{a}_n$ and $\tilde{b}_n$ are the dimensionless version of a_n and b_n with $n = 1, 2, 3, 4, 5, 6$.

With the variational procedure of $\tilde{\mathcal{G}}(\tilde{H}_a^*)$ over the parameters $\tilde{a}_n$ and $\tilde{b}_n$, we obtain a set of equations as

$$\left[48\langle\tilde{x}^4\rangle + \left(\frac{1}{\alpha} - 16\lambda_1\right)\langle\tilde{x}^2\rangle + 3\right]\tilde{a}_1 + \left[48\langle\tilde{x}^3\rangle + \left(\frac{1}{\alpha} - 16\lambda_1\right)\langle\tilde{x}\rangle\right]\tilde{a}_2 + 4\langle\tilde{x}^4\rangle\tilde{a}_3 + 3\langle\tilde{x}^3\rangle\tilde{a}_4 + 2\langle\tilde{x}^2\rangle\tilde{a}_5 + \langle\tilde{x}\rangle\tilde{a}_6 = 16\alpha\langle\tilde{x}^2\rangle,$$

$$\left[48\langle\tilde{x}^3\rangle + \left(\frac{1}{\alpha} - 16\lambda_1\right)\langle\tilde{x}\rangle\right]\tilde{a}_1 + \left[48\langle\tilde{x}^2\rangle + \left(\frac{1}{\alpha} - 16\lambda_1\right)\right]\tilde{a}_2 + 4\langle\tilde{x}^3\rangle\tilde{a}_3 + 3\langle\tilde{x}^2\rangle\tilde{a}_4 + 2\langle\tilde{x}\rangle\tilde{a}_5 + \tilde{a}_6 = 16\alpha\langle\tilde{x}\rangle,$$

$$\frac{\langle\tilde{x}^4\rangle}{\alpha}\tilde{a}_1 + \frac{\langle\tilde{x}^3\rangle}{\alpha}\tilde{a}_2 + 4\langle\tilde{x}^6\rangle\tilde{a}_3 + 3\langle\tilde{x}^5\rangle\tilde{a}_4 + 2\langle\tilde{x}^4\rangle\tilde{a}_5 + \langle\tilde{x}^3\rangle\tilde{a}_6 = 0,$$

$$\frac{\langle\tilde{x}^3\rangle}{\alpha}\tilde{a}_1 + \frac{\langle\tilde{x}^2\rangle}{\alpha}\tilde{a}_2 + 4\langle\tilde{x}^5\rangle\tilde{a}_3 + 3\langle\tilde{x}^4\rangle\tilde{a}_4 + 2\langle\tilde{x}^3\rangle\tilde{a}_5 + \langle\tilde{x}^2\rangle\tilde{a}_6 = 0,$$

$$\frac{\langle\tilde{x}^2\rangle}{\alpha}\tilde{a}_1 + \frac{\langle\tilde{x}\rangle}{\alpha}\tilde{a}_2 + 4\langle\tilde{x}^4\rangle\tilde{a}_3 + 3\langle\tilde{x}^3\rangle\tilde{a}_4 + 2\langle\tilde{x}^2\rangle\tilde{a}_5 + \langle\tilde{x}\rangle\tilde{a}_6 = 0,$$

$$\frac{\langle\tilde{x}\rangle}{\alpha}\tilde{a}_1 + \frac{1}{\alpha}\tilde{a}_2 + 4\langle\tilde{x}^3\rangle\tilde{a}_3 + 3\langle\tilde{x}^2\rangle\tilde{a}_4 + 2\langle\tilde{x}\rangle\tilde{a}_5 + \tilde{a}_6 = 0,$$

$$\left[48\langle\tilde{x}^4\rangle + \left(\frac{1}{\alpha} - 16\lambda_1\right)\langle\tilde{x}^2\rangle + 3\right]\tilde{a}_1 + \left[48\langle\tilde{x}^3\rangle + \left(\frac{1}{\alpha} - 16\lambda_1\right)\langle\tilde{x}\rangle\right]\tilde{a}_2 + 4\langle\tilde{x}^4\rangle\tilde{a}_3 + 3\langle\tilde{x}^3\rangle\tilde{a}_4 + 2\langle\tilde{x}^2\rangle\tilde{a}_5 + \langle\tilde{x}\rangle\tilde{a}_6 = 16\alpha\langle\tilde{x}\rangle,$$

$$\tilde{a}_1 + \left[48\langle\tilde{x}^2\rangle + \left(\frac{1}{\alpha} - 16\lambda_1\right)\right]\tilde{a}_2 + 4\langle\tilde{x}^3\rangle\tilde{a}_3 + 3\langle\tilde{x}^2\rangle\tilde{a}_4 + 2\langle\tilde{x}\rangle\tilde{a}_5 + \tilde{a}_6 = 16\alpha,$$

$$\frac{\langle\tilde{x}^4\rangle}{\alpha}\tilde{a}_1 + \frac{\langle\tilde{x}^3\rangle}{\alpha}\tilde{a}_2 + 4\langle\tilde{x}^6\rangle\tilde{a}_3 + 3\langle\tilde{x}^5\rangle\tilde{a}_4 + 2\langle\tilde{x}^4\rangle\tilde{a}_5 + \langle\tilde{x}^3\rangle\tilde{a}_6 = 0,$$

$$\frac{\langle\tilde{x}^3\rangle}{\alpha}\tilde{a}_1 + \frac{\langle\tilde{x}^2\rangle}{\alpha}\tilde{a}_2 + 4\langle\tilde{x}^5\rangle\tilde{a}_3 + 3\langle\tilde{x}^4\rangle\tilde{a}_4 + 2\langle\tilde{x}^3\rangle\tilde{a}_5 + \langle\tilde{x}^2\rangle\tilde{a}_6 = 0,$$

$$\frac{\langle\tilde{x}^2\rangle}{\alpha}\tilde{a}_1 + \frac{\langle\tilde{x}\rangle}{\alpha}\tilde{a}_2 + 4\langle\tilde{x}^4\rangle\tilde{a}_3 + 3\langle\tilde{x}^3\rangle\tilde{a}_4 + 2\langle\tilde{x}^2\rangle\tilde{a}_5 + \langle\tilde{x}\rangle\tilde{a}_6 = 0,$$

$$\frac{\langle\tilde{x}\rangle}{\alpha}\tilde{a}_1 + \frac{1}{\alpha}\tilde{a}_2 + 4\langle\tilde{x}^3\rangle\tilde{a}_3 + 3\langle\tilde{x}^2\rangle\tilde{a}_4 + 2\langle\tilde{x}\rangle\tilde{a}_5 + \tilde{a}_6 = 0, \quad \text{(D4)}$$

where $\langle\tilde{x}^n\rangle \equiv \int_{-\infty}^{+\infty}\tilde{x}^n\exp(-\tilde{U}_o)d\tilde{x}/\int_{-\infty}^{+\infty}\exp(-\tilde{U}_o)d\tilde{x}$ with $n = 1, 2, 3, 4$. We first numerically obtain the values of $\langle\tilde{x}^n\rangle$ for different values of control parameters λ_1 and λ_2. According to the boundary conditions of λ_1 and λ_2, we set the range of control parameters to be $\lambda_1 \in [-5, 5]$ and $\lambda_2 \in [-5, 5]$. Second, we numerically solve the set of Eq. (D4) for different values of $\langle\tilde{x}^n\rangle$ marked by different set of control parameters λ_1 and λ_2. In this way, we obtain the corresponding solutions of $\tilde{a}_n$ and $\tilde{b}_n$ for different set of control parameters λ_1 and λ_2. Finally, we fit the polynomial relation between the coefficients $\tilde{a}_n$, $\tilde{b}_n$ and the parameters λ_1, λ_2.

The dimensionless auxiliary potential takes the form as

$$\tilde{U}_a(\tilde{X}, s) = \lambda_1'(\tilde{a}_3\tilde{X}^4 + \tilde{a}_4\tilde{X}^3 + \tilde{a}_5\tilde{X}^2 + \tilde{a}_6\tilde{X}) + \lambda_2'(\tilde{b}_3\tilde{X}^4 + \tilde{b}_4\tilde{X}^3 + \tilde{b}_5\tilde{X}^2 + \tilde{b}_6\tilde{X}) + \tilde{C}_2(s)\tilde{X}^2 + \tilde{C}_1(s)\tilde{X}, \tag{D5}$$

where the dimensionless parameters follow as

$$\tilde{C}_2(s) = -\frac{1}{2}\left(\lambda_1''\tilde{a}_1 + \lambda_2''\tilde{b}_1 + \lambda_1'^2\frac{\partial\tilde{a}_1}{\partial\lambda_1} + \frac{1}{\alpha}\lambda_1'^2\tilde{a}_1^2 + \lambda_2'^2\frac{\partial\tilde{b}_1}{\partial\lambda_2} + \frac{1}{\alpha}\lambda_2'^2\tilde{b}_1^2 + \lambda_1'\lambda_2'\frac{\partial\tilde{a}_1}{\partial\lambda_2} + \lambda_1'\lambda_2'\frac{\partial\tilde{b}_1}{\partial\lambda_1} + \frac{2}{\alpha}\lambda_1'\lambda_2'\tilde{a}_1\tilde{b}_1\right),$$

$$\tilde{C}_1(s) = -\left(\lambda_1''\tilde{a}_2 + \lambda_2''\tilde{b}_2 + \lambda_1'^2\frac{\partial\tilde{a}_2}{\partial\lambda_1} + \frac{1}{\alpha}\lambda_1'^2\tilde{a}_1\tilde{a}_2 + \lambda_2'^2\frac{\partial\tilde{b}_2}{\partial\lambda_2} + \frac{1}{\alpha}\lambda_2'^2\tilde{b}_1\tilde{b}_2 + \lambda_1'\lambda_2'\frac{\partial\tilde{a}_2}{\partial\lambda_2} + \lambda_1'\lambda_2'\frac{\partial\tilde{b}_2}{\partial\lambda_1} + \frac{1}{\alpha}\lambda_1'\lambda_2'\tilde{a}_2\tilde{b}_1 + \frac{1}{\alpha}\lambda_1'\lambda_2'\tilde{a}_1\tilde{b}_2\right). \tag{D6}$$

2. Dimensionless quadratic form

We take the quadratic form of the auxiliary Hamiltonian in Eq. (C7) into account. The dimensionless variational auxiliary Hamiltonian takes the form as

$$\tilde{H}_a^* = \lambda_1'(\tilde{a}_1\tilde{x}\tilde{p} + \tilde{a}_2\tilde{p} + \tilde{a}_3\tilde{x}^2 + \tilde{a}_4\tilde{x}) + \lambda_2'(\tilde{b}_1\tilde{x}\tilde{p} + \tilde{b}_2\tilde{p} + \tilde{b}_3\tilde{x}^2 + \tilde{b}_4\tilde{x}). \tag{D7}$$

Here the parameters $\tilde{a}_n$ and $\tilde{b}_n$ are the dimensionless variables with $n = 1, 2, 3, 4$.

Following the variational procedure of $\tilde{\mathcal{G}}(\tilde{H}_a^*)$ over the parameters $\tilde{a}_n$ and $\tilde{b}_n$, we derive the set of equations as

$$\left[48\langle\tilde{x}^4\rangle + \left(\frac{1}{\alpha} - 16\lambda_1\right)\langle\tilde{x}^2\rangle + 3\right]\tilde{a}_4 + \left[48\langle\tilde{x}^3\rangle + \left(\frac{1}{\alpha} - 16\lambda_1\right)\langle\tilde{x}\rangle\right]\tilde{a}_3 + 2\langle\tilde{x}^2\rangle\tilde{a}_2 + \langle\tilde{x}\rangle\tilde{a}_1 = 16\alpha\langle\tilde{x}^2\rangle,$$

$$\left[48\langle\tilde{x}^3\rangle + \left(\frac{1}{\alpha} - 16\lambda_1\right)\langle\tilde{x}\rangle\right]\tilde{a}_4 + \left[48\langle\tilde{x}^2\rangle + \left(\frac{1}{\alpha} - 16\lambda_1\right)\right]\tilde{a}_3 + 2\langle\tilde{x}\rangle\tilde{a}_2 + \tilde{a}_1 = 16\alpha\langle\tilde{x}\rangle,$$

$$\frac{\langle\tilde{x}^2\rangle}{\alpha}\tilde{a}_4 + \frac{\langle\tilde{x}\rangle}{\alpha}\tilde{a}_3 + 2\langle\tilde{x}^2\rangle\tilde{a}_2 + \langle\tilde{x}\rangle\tilde{a}_1 = 0,$$

$$\frac{\langle\tilde{x}\rangle}{\alpha}\tilde{a}_4 + \frac{1}{\alpha}\tilde{a}_3 + 2\langle\tilde{x}\rangle\tilde{a}_2 + \tilde{a}_1 = 0,$$

$$\left[48\langle\tilde{x}^4\rangle + \left(\frac{1}{\alpha} - 16\lambda_1\right)\langle\tilde{x}^2\rangle + 3\right]\tilde{b}_4 + \left[48\langle\tilde{x}^3\rangle + \left(\frac{1}{\alpha} - 16\lambda_1\right)\langle\tilde{x}\rangle\right]\tilde{b}_3 + 2\langle\tilde{x}^2\rangle\tilde{b}_2 + \langle\tilde{x}\rangle\tilde{b}_1 = 16\alpha\langle\tilde{x}\rangle,$$

$$\left[48\langle\tilde{x}^3\rangle + \left(\frac{1}{\alpha} - 16\lambda_1\right)\langle\tilde{x}\rangle\right]\tilde{b}_4 + \left[48\langle\tilde{x}^2\rangle + \left(\frac{1}{\alpha} - 16\lambda_1\right)\right]\tilde{b}_3 + 2\langle\tilde{x}\rangle\tilde{b}_2 + \tilde{b}_1 = 16\alpha,$$

$$\frac{\langle\tilde{x}^2\rangle}{\alpha}\tilde{b}_4 + \frac{\langle\tilde{x}\rangle}{\alpha}\tilde{b}_3 + 2\langle\tilde{x}^2\rangle\tilde{b}_2 + \langle\tilde{x}\rangle\tilde{b}_1 = 0,$$

$$\frac{\langle\tilde{x}\rangle}{\alpha}\tilde{b}_4 + \frac{1}{\alpha}\tilde{b}_3 + 2\langle\tilde{x}\rangle\tilde{b}_2 + \tilde{b}_1 = 0. \tag{D8}$$

Solving the set of equations numerically, we obtain $\tilde{a}_n$ and $\tilde{b}_n$ for a different set of control parameters λ_1 and λ_2.

The dimensionless auxiliary potential takes the form as

$$\tilde{U}_a(\tilde{X}, s) = \lambda_1'(\tilde{a}_3\tilde{X}^2 + \tilde{a}_4\tilde{X}) + \lambda_2'(\tilde{b}_3\tilde{X}^2 + \tilde{b}_4\tilde{X}) + \tilde{C}_2(s)\tilde{X}^2 + \tilde{C}_1(s)\tilde{X}, \tag{D9}$$

where the dimensionless parameters follow as

$$\tilde{C}_2(s) = -\frac{1}{2}\left(\lambda_1''\tilde{a}_1 + \lambda_2''\tilde{b}_1 + \lambda_1'^2\frac{\partial\tilde{a}_1}{\partial\lambda_1} + \frac{1}{\alpha}\lambda_1'^2\tilde{a}_1^2 + \lambda_2'^2\frac{\partial\tilde{b}_1}{\partial\lambda_2} + \frac{1}{\alpha}\lambda_2'^2\tilde{b}_1^2 + \lambda_1'\lambda_2'\frac{\partial\tilde{a}_1}{\partial\lambda_2} + \lambda_1'\lambda_2'\frac{\partial\tilde{b}_1}{\partial\lambda_1} + \frac{2}{\alpha}\lambda_1'\lambda_2'\tilde{a}_1\tilde{b}_1\right),$$

$$\tilde{C}_1(s) = -\left(\lambda_1''\tilde{a}_2 + \lambda_2''\tilde{b}_2 + \lambda_1'^2\frac{\partial\tilde{a}_2}{\partial\lambda_1} + \frac{1}{\alpha}\lambda_1'^2\tilde{a}_1\tilde{a}_2 + \lambda_2'^2\frac{\partial\tilde{b}_2}{\partial\lambda_2} + \frac{1}{\alpha}\lambda_2'^2\tilde{b}_1\tilde{b}_2 + \lambda_1'\lambda_2'\frac{\partial\tilde{a}_2}{\partial\lambda_2} + \lambda_1'\lambda_2'\frac{\partial\tilde{b}_2}{\partial\lambda_1} + \frac{1}{\alpha}\lambda_1'\lambda_2'\tilde{a}_2\tilde{b}_1 + \frac{1}{\alpha}\lambda_1'\lambda_2'\tilde{a}_1\tilde{b}_2\right). \tag{D10}$$

APPENDIX E: ILLUSTRATIVE EXAMPLE OF HOW THE ASSUMPTION OF NEGLECTING HIGH-ORDER MOMENTUM TERMS WORKS

This Appendix presents an illustrative example to show how the high-order momentum terms can be neglected.

Consider a Brownian particle controlled by the harmonic potential with the Hamiltonian

$$H_o = \frac{p^2}{2m} + \frac{1}{2}\lambda(t)x^2, \tag{E1}$$

where $\lambda(t)$ represents the time-dependent stiffness. In the shortcut strategy, an auxiliary Hamiltonian

$$H_a = \frac{\dot{\lambda}}{4\gamma\lambda}[(p - \gamma x)^2 + m\lambda x^2] \quad (E2)$$

is introduced to guide the particle's evolution along the instantaneous equilibrium path. To assess the significance of high-order momentum terms, we introduce the characteristic length $x_c \equiv (k_B T/\lambda(0))^{1/2}$, the characteristic times $\tau_1 \equiv m/\gamma$ and $\tau_2 \equiv \gamma/\lambda(0)$ to rescale variables in Eq. (E2) as $\tilde{x} \equiv x/x_c$, $\tilde{p} \equiv \tau_2/(mx_c)$, $s \equiv t/\tau_2$, and $\tilde{\lambda} \equiv \lambda/\lambda(0)$. The dimensionless forms of the original Hamiltonian H_o and the auxiliary Hamiltonian H_a become

$$\tilde{H}_o \equiv \frac{H_o}{k_B T} = \alpha\frac{\tilde{p}^2}{2} + \frac{1}{2}\tilde{\lambda}\tilde{x}^2, \quad (E3)$$

and

$$\tilde{H}_a \equiv \frac{H_a}{k_B T} = \alpha^2\frac{\tilde{\lambda}'}{4\tilde{\lambda}}\tilde{p}^2 - \alpha\left(\frac{\tilde{\lambda}'}{2\tilde{\lambda}}\tilde{x}\tilde{p} - \frac{\tilde{\lambda}'}{4}\tilde{x}^2\right) + \frac{\tilde{\lambda}'}{4\tilde{\lambda}}\tilde{x}^2. \quad (E4)$$

Here $\alpha \equiv m\lambda(0)/\gamma^2$ and $\tilde{\lambda}' \equiv d\tilde{\lambda}/ds$. The order of each term in $\tilde{H}_o$ and $\tilde{H}_a$ varies with α, with only the $\tilde{p}^2$ term in Eq. (E4) being second-order in α. Hence, neglecting the $\tilde{p}^2$ term is feasible when α can be considered small. By definition, $\alpha \equiv m\lambda(0)/\gamma^2$ implies that neglecting these terms is valid when either the particle's mass m or the initial stiffness $\lambda(0)$ is considerably smaller than the dissipation coefficient γ.

APPENDIX F: GEODESIC PATH FOR SHORTCUTS TO MEMORY ERASURE

Within this Appendix, we employ the geometric approach to determine the geodesic path that incurs minimal energy costs for the erasure process governed by the shortcut scheme. By utilizing the variational auxiliary Hamiltonian in Eq. (D3) or Eq. (D7), we obtain the dimensionless metric for the parametric space as

$$\tilde{g} = \begin{pmatrix} \tilde{a}_1^2\langle\tilde{x}^2\rangle + 2\tilde{a}_1\tilde{a}_2\langle\tilde{x}\rangle + \tilde{a}_2^2 & \tilde{a}_1\tilde{b}_1\langle\tilde{x}^2\rangle + (\tilde{a}_2\tilde{b}_1 + \tilde{b}_2\tilde{a}_1)\langle\tilde{x}\rangle + \tilde{a}_2\tilde{b}_2 \\ \tilde{a}_1\tilde{b}_1\langle\tilde{x}^2\rangle + (\tilde{a}_2\tilde{b}_1 + \tilde{b}_2\tilde{a}_1)\langle\tilde{x}\rangle + \tilde{a}_2\tilde{b}_2 & \tilde{b}_1^2\langle\tilde{x}^2\rangle + 2\tilde{b}_1\tilde{b}_2\langle\tilde{x}\rangle + \tilde{b}_2^2 \end{pmatrix}. \quad (F1)$$

The polynomial relation between the metric $\tilde{g}_{\mu\nu}$ and the parameters λ_1 and λ_2 is established by substituting the values of $\tilde{a}_n$, $\tilde{b}_n$, and $\langle\tilde{x}^n\rangle$ into Eq. (F1).

According to the geometric approach presented in the main text, the task of finding optimal erasure protocol with minimal energy costs is equivalent to solving the geodesic path within the parametric space with the metric $\tilde{g}_{\mu\nu}$. The geodesic path is obtained by solving the geodesic equation

$$\ddot{\lambda}_\mu + \sum_{\nu\kappa}\Gamma^\mu_{\nu\kappa}\dot{\lambda}_\nu\dot{\lambda}_\kappa = 0, \quad (F2)$$

subject to the given boundary conditions $\vec{\lambda}(0) = (1, 0)$ and $\vec{\lambda}(\tau) = (0, 1)$. Here the Christoffel symbol is defined as $\Gamma^\mu_{\nu\kappa} \equiv \frac{1}{2}\sum_\iota(\tilde{g}^{-1})_{\iota\mu}(\partial_{\lambda_\kappa}\tilde{g}_{\iota\nu} + \partial_{\lambda_\nu}\tilde{g}_{\iota\kappa} - \partial_{\lambda_\iota}\tilde{g}_{\nu\kappa})$. The numerical solution of the geodesic equation is executed using the shooting method [56]. The two-point boundary values problem is treated as an initial value problem

$$\ddot{\lambda}_\mu = y_\mu(t, \vec{\lambda}, \dot{\vec{\lambda}}) \equiv \frac{1}{2}\sum_{\nu\kappa\iota}(g^{-1})_{\iota\mu}\left(\frac{\partial g_{\nu\kappa}}{\partial\lambda_\iota} - \frac{\partial g_{\iota\nu}}{\partial\lambda_\kappa} - \frac{\partial g_{\iota\kappa}}{\partial\lambda_\nu}\right)\dot{\lambda}_\nu\dot{\lambda}_\kappa, \quad (F3)$$

alongside the initial conditions $\vec{\lambda}(0) = (1, 0)$ and $\dot{\vec{\lambda}}(0+) = \vec{d}$. Here $\vec{d}$ denotes the initial rate, continually adjusted until the solution of Eq. (F3) reaches the desired position $\vec{\lambda}(\tau) = (0, 1)$. In the simulation, the Euler algorithm is employed to solve the geodesic Eq. (F3), and Newton's method is utilized to iterate the initial rate $\vec{d}$ to meet the boundary condition $\vec{\lambda}(\tau) = (0, 1)$.

APPENDIX G: THE STOCHASTIC SIMULATIONS

In this Appendix, we outline the algorithm for simulating the erasure process and deriving the mean work. The dynamics of the memory system are described by the Langevin

equation specified in Eq. (A12). Its dimensionless form is expressed as

$$\tilde{X}' = \tilde{P},$$
$$\tilde{P}' = -\frac{1}{\alpha}\frac{\partial\tilde{U}_o}{\partial\tilde{X}} - \frac{1}{\alpha}\frac{\partial\tilde{U}_a}{\partial\tilde{X}} - \frac{\tilde{P}}{\alpha} + \frac{\sqrt{2}}{\alpha}\zeta(s), \quad (G1)$$

where $\zeta(s)$ represents Gaussian white noise, satisfying $\langle\zeta(s)\rangle = 0$ and $\langle\zeta(s_1)\zeta(s_2)\rangle = \delta(s_1 - s_2)$. The solution to the Langevin Eq. (G1) is obtained using the Euler algorithm:

$$\tilde{X}(s + \delta s) = \tilde{X}(s) + \tilde{P}\delta s,$$
$$\tilde{P}(s + \delta s) = \tilde{P}(s) - \frac{1}{\alpha}\frac{\partial\tilde{U}_o}{\partial\tilde{X}}\delta s - \frac{1}{\alpha}\frac{\partial\tilde{U}_a}{\partial\tilde{X}}\delta s - \frac{\tilde{P}}{\alpha}\delta s + \frac{\sqrt{2\delta s}}{\alpha}\theta(s), \quad (G2)$$

where δs denotes the time step, and $\theta(s)$ is a random number sampled from a Gaussian distribution with zero mean and unit variance. The work along the system's stochastic trajectory is computed as

$$\tilde{w} \equiv \frac{w}{k_B T} = \int_0^1\left(\frac{\partial\tilde{H}_o}{\partial s} + \frac{\partial\tilde{U}_a}{\partial s}\right)ds$$
$$\approx \sum\left(\frac{\partial\tilde{H}_o}{\partial s} + \frac{\partial\tilde{U}_a}{\partial s}\right)\delta s. \quad (G3)$$

In the simulation, parameters are set to $\vec{\lambda}(0) = (1, 0)$, $\vec{\lambda}(\tau) = (0, 1)$, $k_B T = 1$, $\gamma = 1$, and $m = 0.01$. The mean work is obtained by calculating the ensemble average over the trajectory work of 10^5 stochastic trajectories.

APPENDIX H: NUMERICAL RESULTS

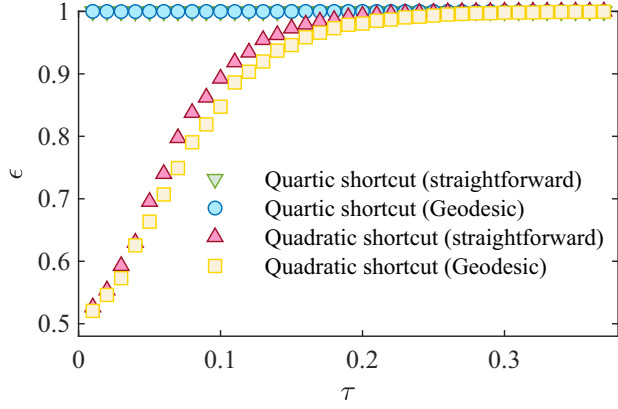In this Appendix, we provide additional numerical results to support the conclusions obtained in the main text.

FIG. 4. The erasure accuracy ϵ of the geodesic protocol compared with the straightforward protocol for different erasure durations τ. During the erasure process, the quartic and the quadratic shortcut schemes are used to carry out the protocols. The erasure accuracy ϵ of the geodesic protocol and that of the straightforward protocol are quite similar for different erasure durations τ. As to the quadratic shortcut scheme, the performance of the straightforward protocol is superior to that of the geodesic protocol.

1. Erasure accuracy of the geodesic protocol

In Appendix F, we derive the geodesic protocol with minimal energy cost for the shortcut to memory erasure employing geometric optimization. Figure 4 shows the erasure accuracy ϵ of the geodesic protocol against the straightforward protocol for different erasure durations τ. We utilize quartic and quadratic shortcut schemes to facilitate memory erasure. Figure 4 illustrates that the erasure accuracy of the geodesic protocol closely mirrors that of the straightforward protocol. For the quadratic shortcut scheme, the performance of the geodesic protocol is slightly inferior to that of the straightforward protocol. These results indicate that while the optimal erasure protocol minimizes energy costs, it doesn't significantly enhance erasure accuracy.

2. Erasure processes controlled by the polynomial protocol

The boundary conditions $\dot{\vec{\lambda}}(0) = \dot{\vec{\lambda}}(\tau) = 0$ are imposed to eliminate the auxiliary control H_a^* at the beginning and end of the erasure process. To satisfy these conditions, we have adopted the straightforward protocol: $\lambda_1^s(t) = 0.5 + 0.5\cos(\pi t/\tau)$ and $\lambda_2^s(t) = 0.5 - 0.5\cos(\pi t/\tau)$. To show that the protocol is not chosen on purpose, we add the erasure process of the polynomial control protocol $\lambda_1^p(t) = 2.0(t/\tau)^3 - 3.0(t/\tau)^2 + 1$ and $\lambda_2^p(t) = -2.0(t/\tau)^3 + 3.0(t/\tau)^2$, commonly employed in shortcuts to adiabaticity [62] to meet the boundary conditions. We elucidate the comparison between these two erasure processes in Fig. 5, contrasting their erasure accuracy and energy cost.

Figures 5(a) and 5(b) depict the erasure accuracy ϵ and the energy cost W_{irr} as a function of erasure duration τ for both the polynomial protocol $\vec{\lambda}^p$ and the straightforward protocol $\vec{\lambda}^s$. In the shortcut to the erasure process, the quartic auxiliary Hamiltonian and the quadratic auxiliary Hamiltonian are respectively applied to carry out the two control protocols. As shown in Fig. 5, there is not much difference between
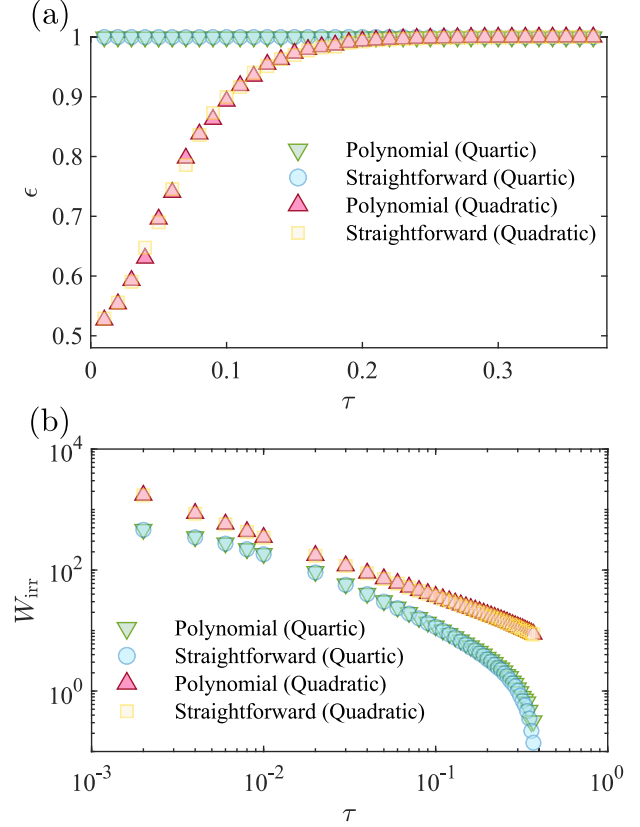

FIG. 5. (a) The erasure accuracy ϵ of the polynomial protocol $\vec{\lambda}^p$ and the straightforward protocol $\vec{\lambda}^s$. The erasure accuracy is defined as the probability of particles ending in the right well $\epsilon \equiv \int_0^\infty dx \int_{-\infty}^{+\infty} dp\, P(x, p, \tau)$. (b) The irreversible energy cost W_{irr} as a function of duration τ for both the polynomial protocol $\vec{\lambda}^p$ and the straightforward protocol $\vec{\lambda}^s$. During the erasure processes, the shortcut schemes adopts the approximate Hamiltonian $H = H_o + H_a^*$ with the auxiliary Hamiltonian H_a^* take the quartic form and the quadratic form, respectively.

the polynomial protocol and the straightforward protocol for the erasure accuracy and the energy cost. This observation underscores that the straightforward protocol $\vec{\lambda}^s$ is presented as a commonly utilized protocol chosen specifically to meet the boundary conditions.

3. Distance between the instantaneous equilibrium path and the approximate shortcut path

To examine the system's evolution during memory erasure, we compare its distribution P with the corresponding equilibrium distribution P_{eq} characterized by the same parameters. The distance between the system's distribution P and the equilibrium distribution P_{eq} are evaluated by using the Jensen-Shannon divergence [63–66]

$$D(P||P_{\text{eq}}) = \frac{1}{2} \int dx\, dp \left(P \ln \frac{2P}{P + P_{\text{eq}}} + P_{\text{eq}} \ln \frac{2P_{\text{eq}}}{P + P_{\text{eq}}} \right).$$
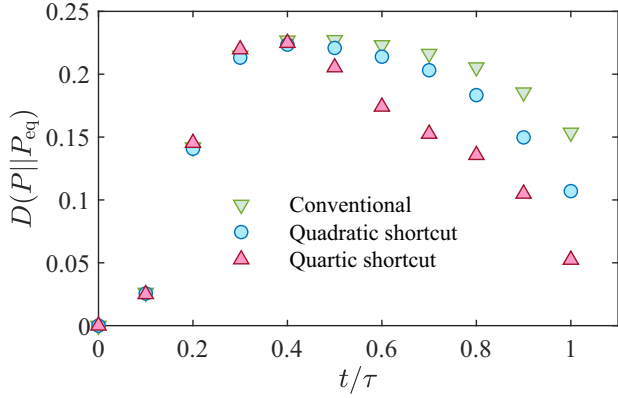(H1)

FIG. 6. The Jensen-Shannon distance [63–66] $D(P||P_{\text{eq}})$ as a function of the evolution time t (lower value means better match). $D(P||P_{\text{eq}})$ evaluates the distance between the system's distribution P and the equilibrium distribution P_{eq}. The memory erasure processes are respectively carried out by the conventional scheme with the Hamiltonian H_o (red triangles), the quadratic shortcut scheme (green squares), and the quartic shortcut scheme (blue circles). In the simulation, we choose the erasure duration to be $\tau = 0.15$.

As shown in Fig. 6, we plot the Jensen-Shannon distance $D(P||P_{\text{eq}})$ against the evolution time t. The memory erasure processes involve the conventional scheme with Hamiltonian H_o (red triangles), the quadratic shortcut scheme (green squares), and the quartic shortcut scheme (blue circles). The erasure duration is chosen to be $\tau = 0.15$. The figure indicates two distinct stages: Initially, when the barrier separating the double well is too significant, the system struggles to reach equilibrium, leading to an increase in distances between P and P_{eq}. Subsequently, thermal fluctuations aid the system in overcoming the lowered barrier, and it follows the instantaneous equilibrium path. For the conventional scheme, the decrease in the Jensen-Shannon distance occurs gradually. However, the addition of the quadratic or quartic auxiliary Hamiltonian significantly expedites this decrease.

Figure 7 illustrates time slices of the system's distribution $P(x, t) = \int P(x, p, t) dp$ during the memory erasure process. As the potential barrier diminishes, the system's distribution P falls behind the instantaneous equilibrium distribution P_{eq}. Nonetheless, the quadratic or quartic shortcut schemes notably accelerate the system's evolution towards the equilibrium path, particularly after the barrier is fully lowered.
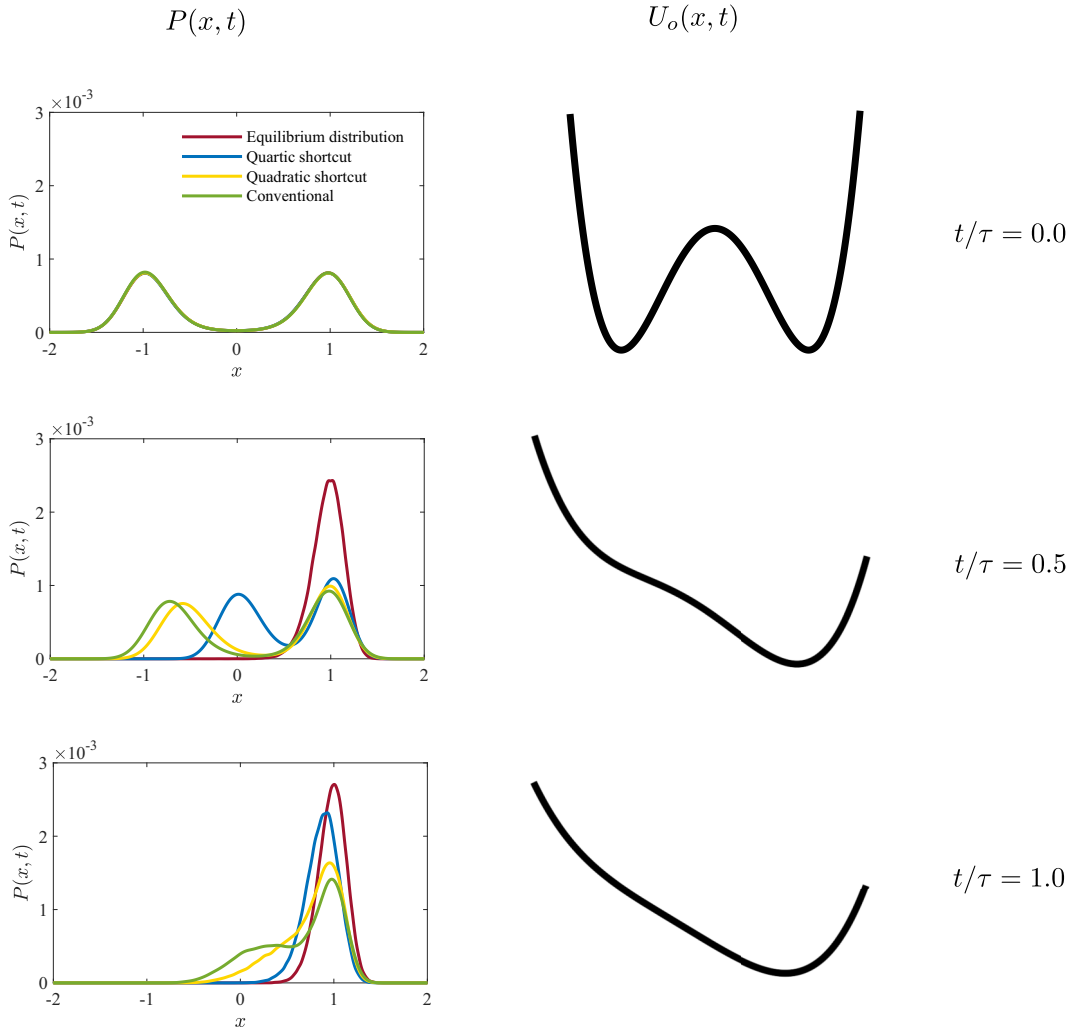

FIG. 7. The left column shows the time slides of the system's distribution during the memory erasure process. The right column shows the evolution of the original potential $U_o(x, t)$. The erasure duration is selected as $\tau = 0.15$.

[1] R. Landauer, IBM J. Res. Dev. **5**, 183 (1961).

[2] C. H. Bennett, IBM J. Res. Dev. **17**, 525 (1973).

[3] J. M. R. Parrondo, J. M. Horowitz, and T. Sagawa, Nat. Phys. **11**, 131 (2015).

[4] D. A. Pearlman and P. A. Kollman, J. Chem. Phys. **91**, 7831 (1989).

[5] R. H. Wood, J. Phys. Chem. **95**, 4838 (1991).

[6] R. Dillenschneider and E. Lutz, Phys. Rev. Lett. **102**, 210601 (2009).

[7] A. Bérut, A. Arakelyan, A. Petrosyan, S. Ciliberto, R. Dillenschneider, and E. Lutz, Nature (London) **483**, 187 (2012).

[8] Y. Jun, M. Gavrilov, and J. Bechhoefer, Phys. Rev. Lett. **113**, 190601 (2014).

[9] A. Bérut, A. Petrosyan, and S. Ciliberto, J. Stat. Mech.: Theory Exp. (2015) P06015.

[10] K. Proesmans, J. Ehrich, and J. Bechhoefer, Phys. Rev. Lett. **125**, 100602 (2020).

[11] K. Proesmans, J. Ehrich, and J. Bechhoefer, Phys. Rev. E **102**, 032105 (2020).

[12] A. B. Boyd, A. Patra, C. Jarzynski, and J. P. Crutchfield, J. Stat. Phys. **187**, 17 (2022).

[13] R. Kawai, J. M. R. Parrondo, and C. van den Broeck, Phys. Rev. Lett. **98**, 080602 (2007).

[14] A. Gomez-Marin, J. M. R. Parrondo, and C. van den Broeck, Phys. Rev. E **78**, 011107 (2008).

[15] S. Vaikuntanathan and C. Jarzynski, Europhys. Lett. **87**, 60005 (2009).

[16] J. Horowitz and C. Jarzynski, Phys. Rev. E **79**, 021106 (2009).

[17] G. Diana, G. B. Bagci, and M. Esposito, Phys. Rev. E **87**, 012111 (2013).

[18] P. R. Zulkowski and M. R. DeWeese, Phys. Rev. E **89**, 052140 (2014).

[19] P. R. Zulkowski and M. R. DeWeese, Phys. Rev. E **92**, 032113 (2015).

[20] S. Dago, J. Pereda, N. Barros, S. Ciliberto, and L. Bellon, Phys. Rev. Lett. **126**, 170601 (2021).

[21] T. van Vu and K. Saito, Phys. Rev. Lett. **128**, 010602 (2022).

[22] Y.-H. Ma, J.-F. Chen, C. P. Sun, and H. Dong, Phys. Rev. E **106**, 034112 (2022).

[23] A. Rolandi, P. Abiuso, and M. Perarnau-Llobet, Phys. Rev. Lett. **131**, 210401 (2023).

[24] M. A. Miller and W. P. Reinhardt, J. Chem. Phys. **113**, 7035 (2000).

[25] C. Jarzynski, Phys. Rev. E **65**, 046122 (2002).

[26] S. Vaikuntanathan and C. Jarzynski, Phys. Rev. Lett. **100**, 190601 (2008).

[27] D. D. L. Minh, J. Chem. Phys. **130**, 204102 (2009).

[28] I. A. Martínez, A. Petrosyan, D. Guéry-Odelin, E. Trizac, and S. Ciliberto, Nat. Phys. **12**, 843 (2016).

[29] A. Patra and C. Jarzynski, New J. Phys. **19**, 125009 (2017).

[30] G. Li, H. T. Quan, and Z. C. Tu, Phys. Rev. E **96**, 012144 (2017).

[31] A. Deshpande, M. Gopalkrishnan, T. E. Ouldridge, and N. S. Jones, Proc. R. Soc. A **473**, 20170117 (2017).

[32] J. Sanders, M. Baldovin, and P. Muratore-Ginanneschi, arXiv:2403.00679 (2024).

[33] E. Aurell, C. Mejía-Monasterio, and P. Muratore-Ginanneschi, Phys. Rev. Lett. **106**, 250601 (2011).

[34] E. Aurell, K. Gawęczki, C. Mejía-Monasterio, R. Mohayaee, and P. Muratore-Ginanneschi, J. Stat. Phys. **147**, 487 (2012).

[35] Y. Zhang, Europhys. Lett. **128**, 30002 (2020).

[36] S. Dago and L. Bellon, Phys. Rev. Lett. **128**, 070604 (2022).

[37] J. A. C. Albay, S. R. Wulaningrum, C. Kwon, P.-Y. Lai, and Y. Jun, Phys. Rev. Res. **1**, 033122 (2019).

[38] J. A. C. Albay, P.-Y. Lai, and Y. Jun, Appl. Phys. Lett. **116**, 103706 (2020).

[39] G. Li and Z. C. Tu, Phys. Rev. E **100**, 012127 (2019).

[40] G. Li and Z. C. Tu, Phys. Rev. E **103**, 032146 (2021).

[41] I. A. Martínez, É. Roldán, L. Dinis, and R. A. Rica, Soft Matter **13**, 22 (2017).

[42] C. A. Plata, D. Guéry-Odelin, E. Trizac, and A. Prados, J. Stat. Mech.: Theory Exp. (2020) 093207.

[43] J.-F. Chen, Phys. Rev. E **106**, 054108 (2022).

[44] X.-H. Zhao, Z.-N. Gong, and Z. C. Tu, Phys. Rev. E **106**, 064117 (2022).

[45] G. Li, J.-F. Chen, C. P. Sun, and H. Dong, Phys. Rev. Lett. **128**, 230603 (2022).

[46] G. Li, C. P. Sun, and H. Dong, Phys. Rev. E **107**, 014103 (2023).

[47] S. S. Chittari and Z. Lu, J. Chem. Phys. **159**, 084106 (2023).

[48] K. Maruyama, F. Nori, and V. Vedral, Rev. Mod. Phys. **81**, 1 (2009).

[49] J. Bechhoefer, *Control Theory for Physicists* (Cambridge University Press, Cambridge, 2020).

[50] P. Salamon and R. S. Berry, Phys. Rev. Lett. **51**, 1127 (1983).

[51] G. E. Crooks, Phys. Rev. Lett. **99**, 100602 (2007).

[52] D. A. Sivak and G. E. Crooks, Phys. Rev. Lett. **108**, 190602 (2012).

[53] J.-F. Chen, C. P. Sun, and H. Dong, Phys. Rev. E **104**, 034117 (2021).

[54] D. Guéry-Odelin, A. Ruschhaupt, A. Kiely, E. Torrontegui, S. Martínez-Garaot, and J. G. Muga, Rev. Mod. Phys. **91**, 045001 (2019).

[55] D. Guéry-Odelin, C. Jarzynski, C. A. Plata, A. Prados, and E. Trizac, Rep. Prog. Phys. **86**, 035902 (2023).

[56] M. Berger, *A Panoramic View of Riemannian Geometry* (Springer, Berlin, Heidelberg, 2007).

[57] M. Gavrilov and J. Bechhoefer, Phys. Rev. Lett. **117**, 200601 (2016).

[58] D. Raynal, T. de Guillebon, D. Guéry-Odelin, E. Trizac, J.-S. Lauret, and L. Rondin, Phys. Rev. Lett. **131**, 087101 (2023).

[59] C. Jarzynski, Phys. Rev. Lett. **78**, 2690 (1997).

[60] K. Sekimoto and S.-i. Sasa, J. Phys. Soc. Jpn. **66**, 3326 (1997).

[61] L. E. Reichl, *A Modern Course in Statistical Physics* (Wiley, New York, 1998).

[62] A. del Campo, Phys. Rev. Lett. **111**, 100502 (2013).

[63] J. Lin, IEEE Trans. Inf. Theory **37**, 145 (1991).

[64] D. Endres and J. Schindelin, IEEE Trans. Inf. Theory **49**, 1858 (2003).

[65] A. Majtey, P. W. Lamberti, M. T. Martin, and A. Plastino, Eur. Phys. J. D **32**, 413 (2005).

[66] E. H. Feng and G. E. Crooks, Phys. Rev. Lett. **101**, 090602 (2008).